ADD

Interaction Notes

Note 403

January 1981

CABLE SHIELDS WITH PERIODIC BONDINGS

F.C. Yang

The Dikewood Corporation
Santa Monica, California 90405

Abstract

A two-surface cable shield with periodic bondings and excited either discretely or distributedly is analyzed. It is found that the bondings improve the overall shielding effectiveness of the cable shield at certain frequencies, but degrade the shielding at others. Certain criteria are established for better shielding. In the case of distributed excitation, the overall effective transfer functions of a two-surface cable shield can be calculated from simple circuits. These circuits can be extended for multi-surface cable shields.

PREFACE

The author would like to thank Dr. K.S.H. Lee of The Dikewood Corporation, Dr. C.E. Baum and Mr. W. Kehrer of the Air Force Weapons Laboratory (AFWL) for helpful discussions and suggestions, and Mr. V. Tatoian of Dikewood for numerical computations.

CONTENTS

TABLES

ILLUSTRATIONS

ILLUSTRATIONS (CONTINUED)

I. INTRODUCTION

Cable shields and cable conduits have been widely used as part of the integrated EMP hardening design for aircraft, missiles and ground-based systems (e.g. see Ref. 1). When cable shields are used over a long distance, they are generally periodically grounded to their immediate outer shield through bonding straps, clamps, screws, etc. The periodic grounding provides mechanical rigidity of the shields, reduces the electrostatic hazards, and at the same time might increase the shielding effectiveness against penetration of long-wavelength disturbances. However, for the broad-band EMP, the question arises whether the periodic grounding will improve or degrade the overall shielding effectiveness. In this report, this question will be answered from a rigorous theoretical analysis. The analytical results will help the system engineers to determine the optimum grounding arrangement.

Cable shields generally are not perfect. EMP can penetrate either locally (such as through an aperture, a connector, or one end of the shield, see Fig. 1) or distributedly (such as through diffusion or uniformly distributed apertures, see Fig. 2). These two distinct cases will be separately discussed: discrete excitations in Section II and distributed excitations in Section III. Finally, the results obtained in Sections II and III will be summarized in Section IV, and several practical engineering examples as to how the results can be used will be presented.

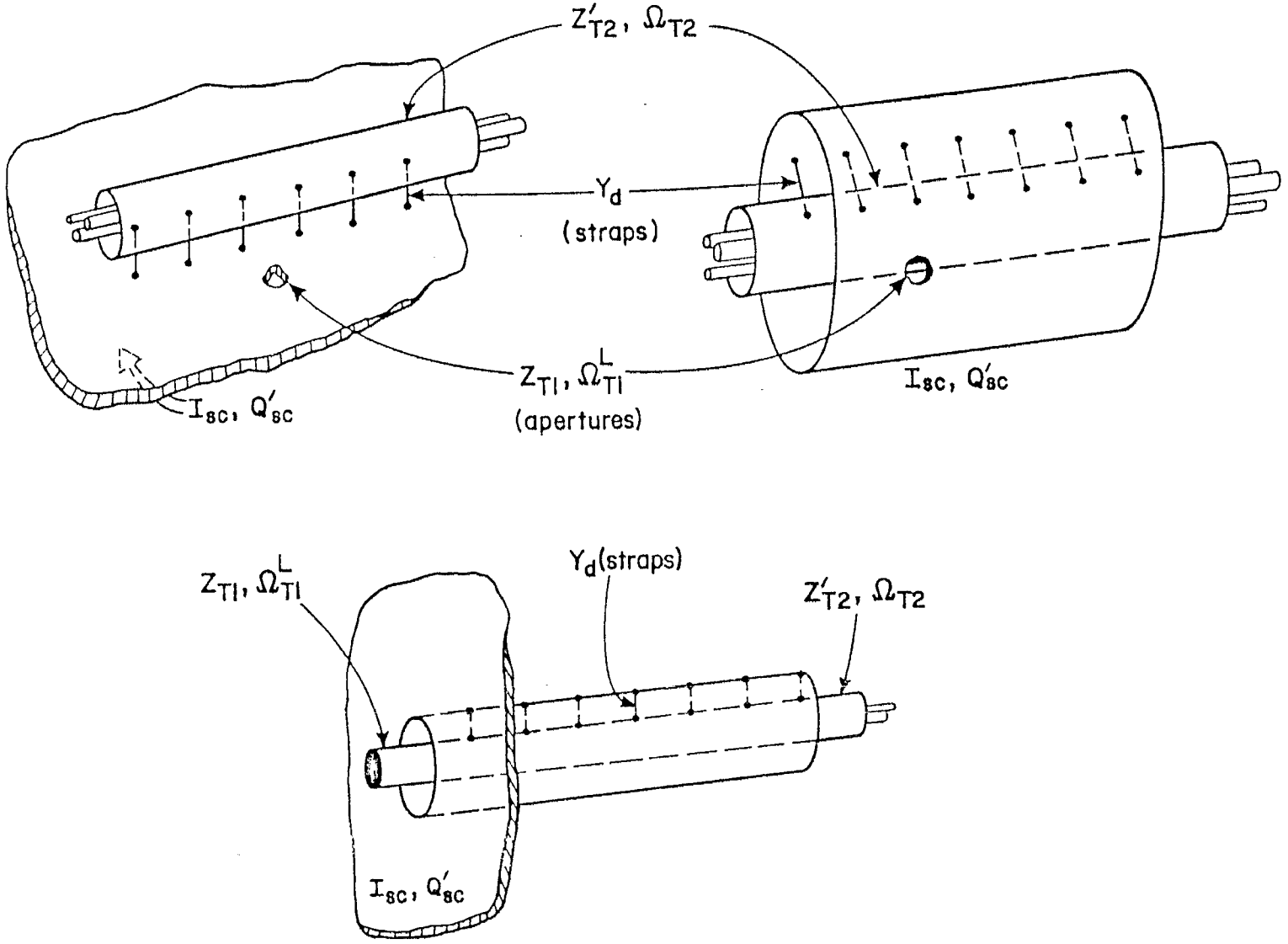

Figure 1. Discretely excited cable shields with periodic bondings.

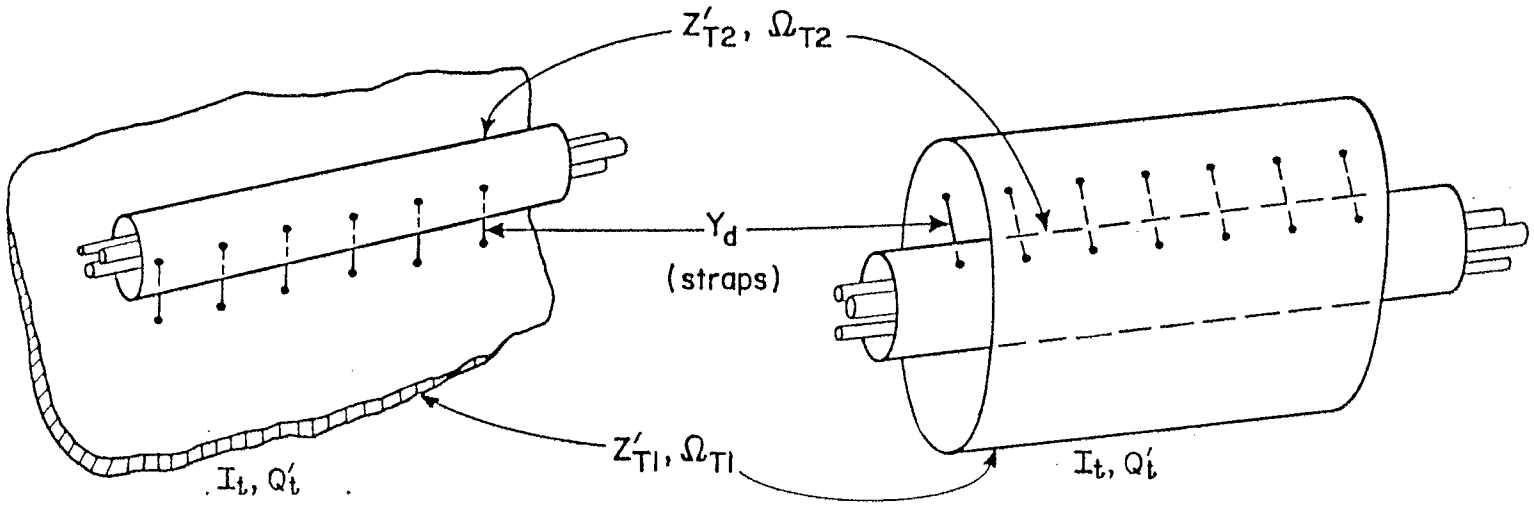

Figure 2. Distributedly excited cable shields with periodic bondings.

II. DISCRETE EXCITATIONS

In this section, the outer shield of a double-shield configuration (see Fig. 1) is assumed to be perfect, except at some isolated locations where the EMP can penetrate. The current and charge density distributions on the transmission line formed by the two shields due to the penetration from a localized location can be calculated by solving the problem depicted in Figure 3. The distributions due to the voltage and current sources of the localized penetration can be separately considered. The two problems of Figure 3a can be decomposed further (see Fig. 4) so that only the problem shown in Figure 3b (which is redrawn as Fig. 5 with $V^s = V_1^s, V_2^s$ or V_o^s and $I^s = I_1^s, I_2^s$ or I_o^s) need be solved. The coupling to the wires inside the inner shield can then be calculated by multiplying the appropriate transfer impedance or charge transfer frequency of the inner shield and the current and charge density distributions. The time variation of $\exp(j\omega t)$ will be assumed and suppressed throughout this report.

At sufficiently low frequencies the TEM mode is dominant and the voltage (V) and current (I) distributions along the line shown in Figure 5 can be calculated by solving the following pair of equations:

$$\frac{dV}{dz} + Z_1' I = 0 \tag{1}$$

$$\frac{dI}{dz} + \left[Y_1' + Y_d \sum_{n=-\infty}^{\infty} \delta(z - nd) \right] V = 0, \qquad \text{for } z \geq z_o \tag{2}$$

where Z_1' and Y_1' are, respectively, the series impedance and shunt admittance per unit length of the line and Y_d is the admittance of each strap.

From Floquet's theorem, the solution of the periodic Equations 1 and 2 has the following form:

$$V(z) = \sum_{n=-\infty}^{\infty} V_n \exp[-j(k + 2n\pi/d)z] \tag{3}$$

$$I(z) = \sum_{n=-\infty}^{\infty} I_n \exp[-j(k + 2n\pi/d)z] \tag{4}$$

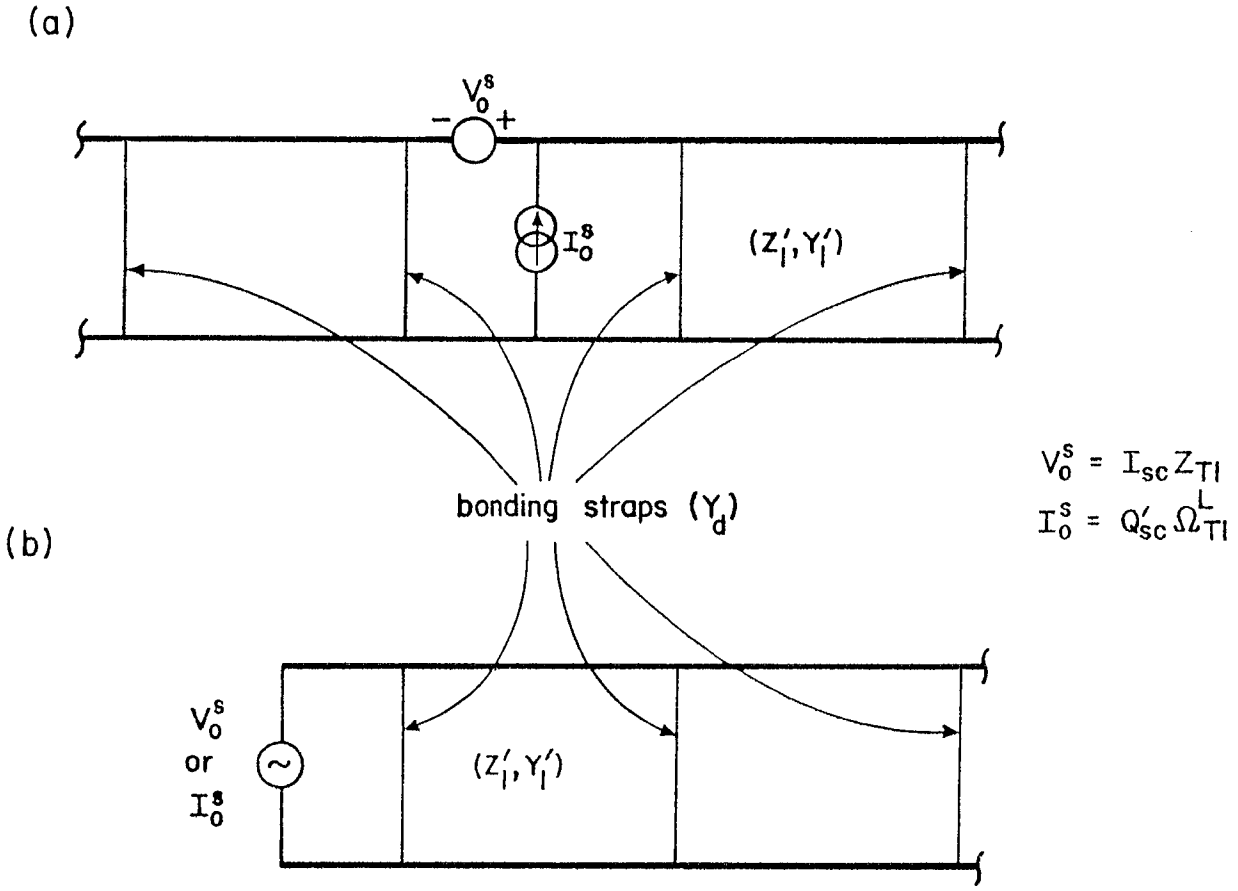

Figure 3. Transmission-line models for discretely excited cable shields with periodic bondings.

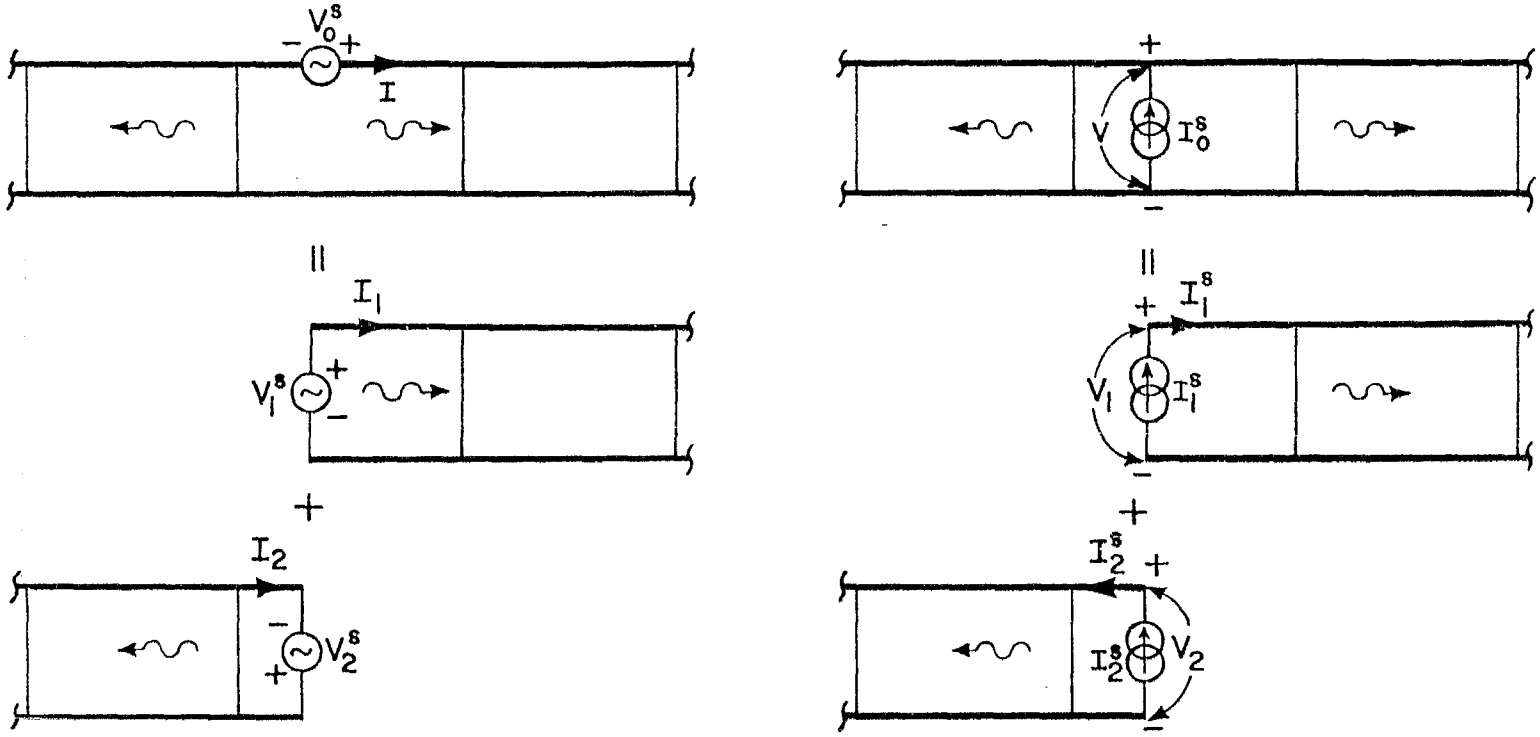

$V_1^s + V_2^s = V_o^s$

$I_1 = I_2 = I$

(a)

$I_1^s + I_2^s = I_o^s$

$V_1 = V_2 = V$

(b)

Figure 4. The decomposition of the problem depicted in Figure 3a.

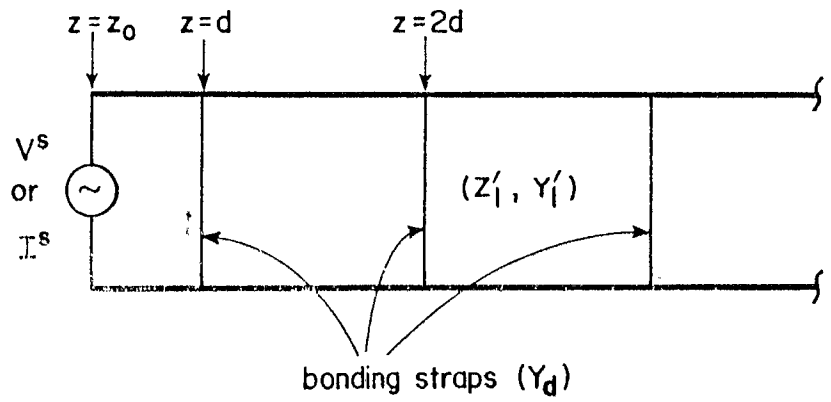

Figure 5. The resultant transmission-line problem to be solved after decomposition.

Substituting Equations 3,4 into Equations 1,2 one has

$$I_n = j\, V_n (k + 2n\pi/d)/Z_1' \tag{5}$$

$$V_n = \frac{-Y_d Z_1'}{Y_1' Z_1' + (k + 2n\pi/d)^2 \cdot d} \frac{V^o}{d} \tag{6}$$

where

$$V^o = \sum_{n=-\infty}^{\infty} V_n \tag{7}$$

By combining Equations 6 and 7, one finds that the dispersion relation between k and $\sqrt{-Y_1'Z_1'}$ is (also see Ref. 2)

$$\cos kd = \cos(d\sqrt{-Y_1'Z_1'}) + \frac{Z_1'Y_d d}{2d\sqrt{-Y_1'Z_1'}} \sin(d\sqrt{-Y_1'Z_1'}) \tag{8}$$

In Figure 6, cos kd is plotted versus $d\sqrt{-Y_1'Z_1'}$ ($\simeq \omega d/c$) for various q_S ($= Z_1'Y_d d$). (Generally, Z_1', Y_1' and Y_d are complex values. To have real and positive $d\sqrt{-Y_1'Z_1'}$ and $Z_1'Y_d d$, one can assume $Z_1' \simeq Z_{c1}'$, $Y_1' \simeq Y_{c1}'$ and $Y_d \simeq (j\omega L_d)^{-1}$, where Z_{c1}' and Y_{c1}' are purely imaginary and are respectively the values of Z_1' and Y_1' of a perfect double shield, L_d is the inductance of each bonding strap). In the figure, one clearly sees the passband and stopband structures. The stopbands are generally broader for a larger q_S, especially at the lower $\omega d/c$ region. This is reasonable because a larger q_S means a better grounding. At the higher $\omega d/c$ region, the stopbands become narrower because the high-frequency disturbance does not see the presence of the bonding straps. Also, to have the proper propagation and decaying constants for $z \geq z_o$, one should restrict the k-value to have a positive real part and a negative imaginary part. The imaginary part of k determines how fast the disturbance decays when it propagates away from the penetration point. A plot of $|\mathrm{Im}(kd)|$ versus frequency for various q_S is given in Figure 7. From the figure, it obviously shows that a larger q_S gives a larger $|\mathrm{Im}(kd)|$ (which means

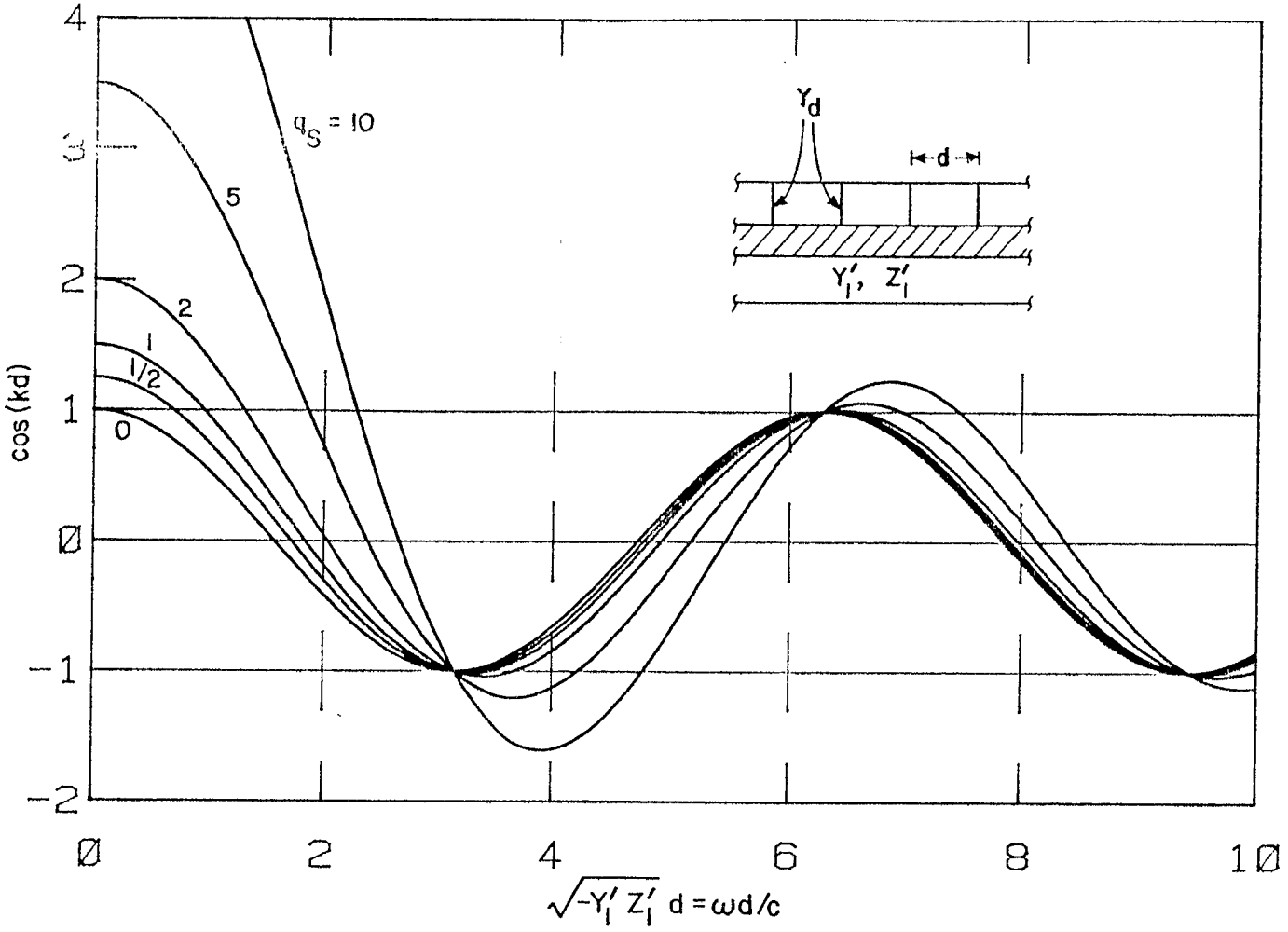

Figure 6. The dispersion relations between ω and k for periodically bonded transmission lines with various $q_S = Z_1' Y_d d$.

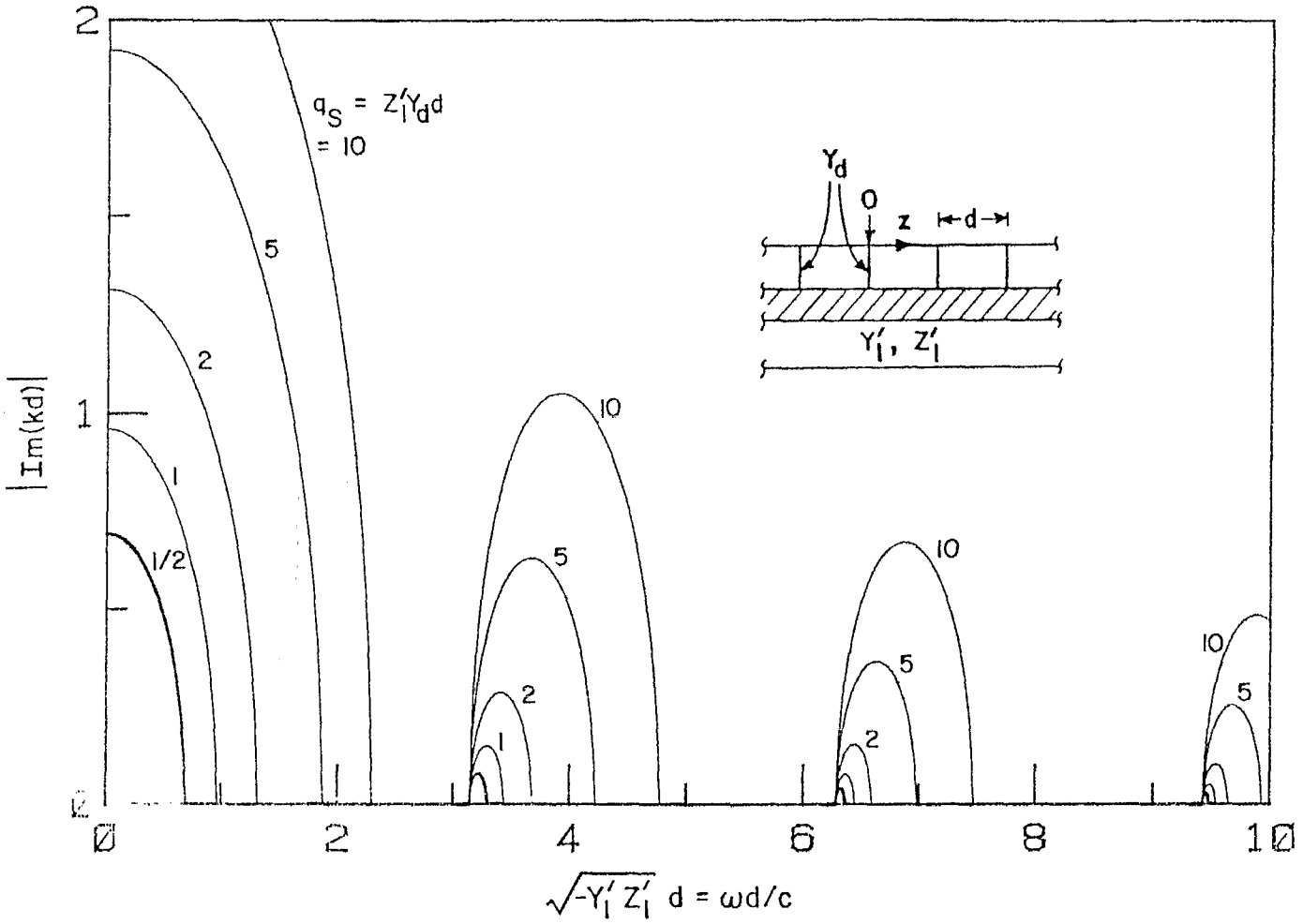

Figure 7. The decaying constants of bonded transmission lines versus frequency for various $q_S = Z_1' Y_d d$.

that the disturbance decays faster) and thus, is more desirable. Actually, at the low-frequency limit where $\sqrt{-Y_1'Z_1'}\, d \approx \omega d/c << 1$, one can easily show that

$$|\mathrm{Im}(kd)| \approx \cosh^{-1}(1 + q_s/2) \tag{9}$$

$$\approx \cosh^{-1}[1 + L_1' d/(2L_d)] \tag{10}$$

where L_1' is the series inductance per unit length of the double shield.

Using Equations 5 and 6 in Equations 3 and 4, one has

$$V(z) = V_o \sum_{n=-\infty}^{\infty} \frac{(Y_1'Z_1' + k^2)}{Y_1'Z_1' + (k + 2n\pi/d)^2} e^{-j(k + 2n\pi/d)z}$$

$$= \frac{-V_o(Y_1'Z_1' + k^2)d^2}{Y_d Z_1' d} e^{-jkd(m+1/2)} \times$$

$$\times \left\{ \frac{\cos(kd/2)\cos\left[\left((m+1/2)d - z \right)\sqrt{-Y_1'Z_1'} \right]}{\cos(d\sqrt{-Y_1'Z_1'}/2)} \right.$$

$$\left. + j \frac{\sin(kd/2)\sin\left[\left((m+1/2)d - z \right)\sqrt{-Y_1'Z_1'} \right]}{\sin(d\sqrt{-Y_1'Z_1'}/2)} \right\} \tag{11}$$

$$\text{for } md \leq z < (m+1)d$$

$$I(z) = V_o \sum_{n=-\infty}^{\infty} \frac{j(Y_1'Z_1' + k^2)}{Y_1'Z_1' + (k + 2n\pi/d)^2} \frac{k + 2n\pi/d}{Z_1'} e^{-j(k + 2n\pi/d)z}$$

$$= \frac{-j\, V_o\, d\sqrt{-Y_1'Z_1'}(k^2 + Y_1'Z_1')d^2}{(dY_d Z_1')Z_1' d} e^{-jkd(m+1/2)} \times$$

$$\times \left\{ \frac{\sin(kd/2)\cos\left[\left((m+1/2)d - z \right)\sqrt{-Y_1'Z_1'} \right]}{\sin(d\sqrt{-Y_1'Z_1'}/2)} \right.$$

$$+ j \frac{\cos(kd/2)\sin\left[\left((m+1/2)d - z\right)\sqrt{-Y_1'Z_1'}\right]}{\cos(d\sqrt{-Y_1'Z_1'}/2)} \Bigg\} \quad \text{for } md \leq z < (m+1)d \tag{12}$$

$$= -\frac{1}{Z_1'}\frac{d}{dz}V(z)$$

To obtain Equations 11 and 12, one has used the dispersion relation 8 and several series summation formulas in Reference 3. With the expression for I(z), one can calculate the total charge per unit length of the double shield from

$$Q'(z) = -\frac{1}{j\omega}\frac{d}{dz}I(z) \tag{13}$$

As is obvious from Equations 11 and 12, V_o is yet to be determined from the boundary condition at $z = z_o$. In what follows, the cases with the voltage and current sources will be considered separately.

1. VOLTAGE SOURCE

Applying the condition that $V = V^s$ at $z = z_o$, one immediately obtains from Equation 11 that

$$V_o = \frac{-Z_1'Y_d\, V^s}{(k^2 + Y_1'Z_1')d}\, e^{jkd/2} \times$$

$$\times \left\{ \frac{\cos(kd/2)\cos[(z_o - d/2)\sqrt{-Y_1'Z_1'}]}{\cos(d\sqrt{-Y_1'Z_1'}/2)} \right.$$

$$\left. - j\frac{\sin(kd/2)\sin[(z_o - d/2)\sqrt{-Y_1'Z_1'}}{\sin(d\sqrt{-Y_1'Z_1'}/2)} \right\}^{-1} \tag{14}$$

The voltage, current and charge distributions of the double shield can be fully expressed by Equations 8, 11, 12, 13 and 14 provided V^s is known. For the problem of Figure 3b, V^s is simply V^s_o. However, to obtain V^s (Note, one uses $V^s = V^s_1$ for $z > z_o$ and $V^s = V^s_2$ for $z < z_o$) for the problem of Figure 4a, one needs to go through some complicated algebraic manipulations involving Equations12 and 14 and the relationships given in Figure 4a. For the special cases of $z_o = 0$ and $d/2$ which are the cases to be considered in the following discussions, $V^s = V^s_1 = V^s_2 = V^s_o/2$. V^s_o can, generally, be obtained from the short-circuit current I_{sc} at the outermost surface of the double shield and the transfer impedance Z_{T1} of the outer shield via

$$V^s_o = I_{sc} Z_{T1} \tag{15}$$

Since $I(z)$ and $Q'(z)$ are now known, one can begin to discuss the coupling to the wires inside the inner shield. The coupling can be completely described by $V'_s(z)$ and $I'_s(z)$ which are, respectively, the voltage and current source terms of the transmission-line equations of the inside cables. If the inner shield has a shield transfer impedance per unit length Z'_{T2} and a charge transfer frequency Ω_{T2}, then, V'_s and I'_s can be calculated from (see Ref. 4):

$$V'_s(z) = Z'_{T2} I(z) \tag{16}$$

$$I'_s(z) = \Omega_{T2} Q'(z) \tag{17}$$

With the above expressions one can then define an effective transfer impedance per unit length Z'_{TV} and an effective charge transfer frequency per unit length Ω'_{TV} for the double shield as follows:

$$Z'_{TV}(z) = V'_s(z)/I_{sc} \tag{18}$$

$$\Omega'_{TV}(z) = j\omega\, I'_s(z)/I_{sc} \tag{19}$$

Here, the subscript "V" is used to indicate that the quantities are for a localized "voltage" source which is generated by I_{sc}.

The two quantities Z'_{TV} and Ω'_{TV} are z-dependent. When the frequencies are in the stopbands, they become extremely small for $z >> z_o$ (see the exponentially decaying term in Equation 12). On the other hand, when the frequencies are inside the passbands, they are oscillatory functions of z and are modulated by the periodicity of the bondings. It, thus, appears that in order to better quantify the coupling to the wires inside the inner shield, one should apply some average schemes to Z'_{TV} and Ω'_{TV} over the period d. A natural scheme is to define

$$\begin{pmatrix} \overline{Z}'_{TV} \\ \overline{\Omega}'_{TV} \end{pmatrix} = \frac{1}{d} \int_{md}^{(m+1)d} \begin{pmatrix} Z'_{TV}(z) \\ \Omega'_{TV}(z) \end{pmatrix} e^{jkz} dz \tag{20}$$

where $n\pi \leq kd < (n+1)\pi$ when $n\pi \leq \sqrt{-Y'_1 Z'_1}\, d < (n+1)\pi$, $n = 0,1,2, \ldots$. These two average quantities are calculated to be

$$\overline{Z}'_{TV} \Big/ \left(\frac{Z_{T1} Z'_{T2}}{n_p \sqrt{Z'_1/Y'_1}} \right) = \overline{\Omega}'_{TV} \Big/ \left(\frac{\Omega_{T2} Z_{T1} Y'_1}{n_p} \right) \cdot \frac{\sqrt{-Y'_1 Z'_1}\, d}{kd}$$

$$= \frac{-(Z'_1 Y_d d)(kd)\exp(jkd/2)}{(\sqrt{-Z'_1 Y'_1}\, d)(k^2 + Y'_1 Z'_1) d^2} \times$$

$$\times \left\{ \frac{\cos(kd/2)\cos[(z_o - d/2)\sqrt{-Z'_1 Y'_1}]}{\cos(d\sqrt{-Z'_1 Y'_1}/2)} \right.$$

$$\left. - j \frac{\sin(kd/2)\sin[(z_o - d/2)\sqrt{-Z'_1 Y'_1}]}{\sin(d\sqrt{-Z'_1 Y'_1}/2)} \right\}^{-1} \tag{21}$$

where $n_p = 1$ for Figure 3b and $n_p = 2$ for Figure 3a.

$\bar{Z}'_{TV}$ and $\bar{\Omega}'_{TV}$ still depend on where $z = z_o$ is. However, no matter what z_o is, one can easily observe that the normalized $|\bar{Z}'_{TV}|$ and $|\bar{\Omega}'_{TV}|$ (normalized with respect to their values when there is no bonding, which are, respectively, $Z_{T1}Z'_{T2}/(n_p\sqrt{Z'_1/Y'_1})$ and $Z_{T1}\Omega_{T2}Y'_1/n_p$) are greater than unity for some regions of $\sqrt{-Z'_1Y'_1}\,d$ ($\simeq \omega d/c$) and smaller than unity for the others. That is, the bondings improve the shielding effectiveness of the double shield at certain frequencies but degrade it at the others. Plots of the normalized $|\bar{Z}'_{TV}|$ and $|\bar{\Omega}'_{TV}|$ for $z_o = 0$ and $d/2$ as functions of $\sqrt{-Z'_1Y'_1}\,d$ and q_S ($= Z'_1Y_d d$) are given in Figures 8 through 11. In the figures, the curves are not given for the stopbands. In the stopbands, the normalized quantities are exponentially decayed away from the penetration point. Since the ranges of the stopbands increase with q_S, one should try to have q_S as large as possible for better shielding effectiveness. This can be achieved by making Z'_1Y_d ($\simeq L'_1/L_d$) large. Note that making "d" large, although increasing q_S, widens $\omega d/c$ and hence narrows the stopbands. From the figures, one also sees that arranging the bondings with $d \simeq cn\pi/\omega$ (where resonances occur) seriously degrades the shielding effectiveness, and thus should be avoided for the important parts of the EMP spectrum.

2. CURRENT SOURCE

Applying the boundary condition that $I = I^s$ at $z = z_o$, one obtains from Equation 12:

$$V_o = \frac{j\, I^s (dY_d Z'_1) Z'_1 d}{d\sqrt{-Y'_1Z'_1}\,(k^2 + Y'_1Z'_1)d^2}\, e^{jkd/2} \times$$

$$\times \left\{ \frac{\sin(kd/2)\cos[(z_o - d/2)\sqrt{-Y'_1Z'_1}]}{\sin(d\sqrt{-Y'_1Z'_1}/2)} \right.$$

$$\left. - j\, \frac{\cos(kd/2)\sin[(z_o - d/2)\sqrt{-Y'_1Z'_1}]}{\cos(d\sqrt{-Y'_1Z'_1}/2)} \right\}^{-1} \qquad (22)$$

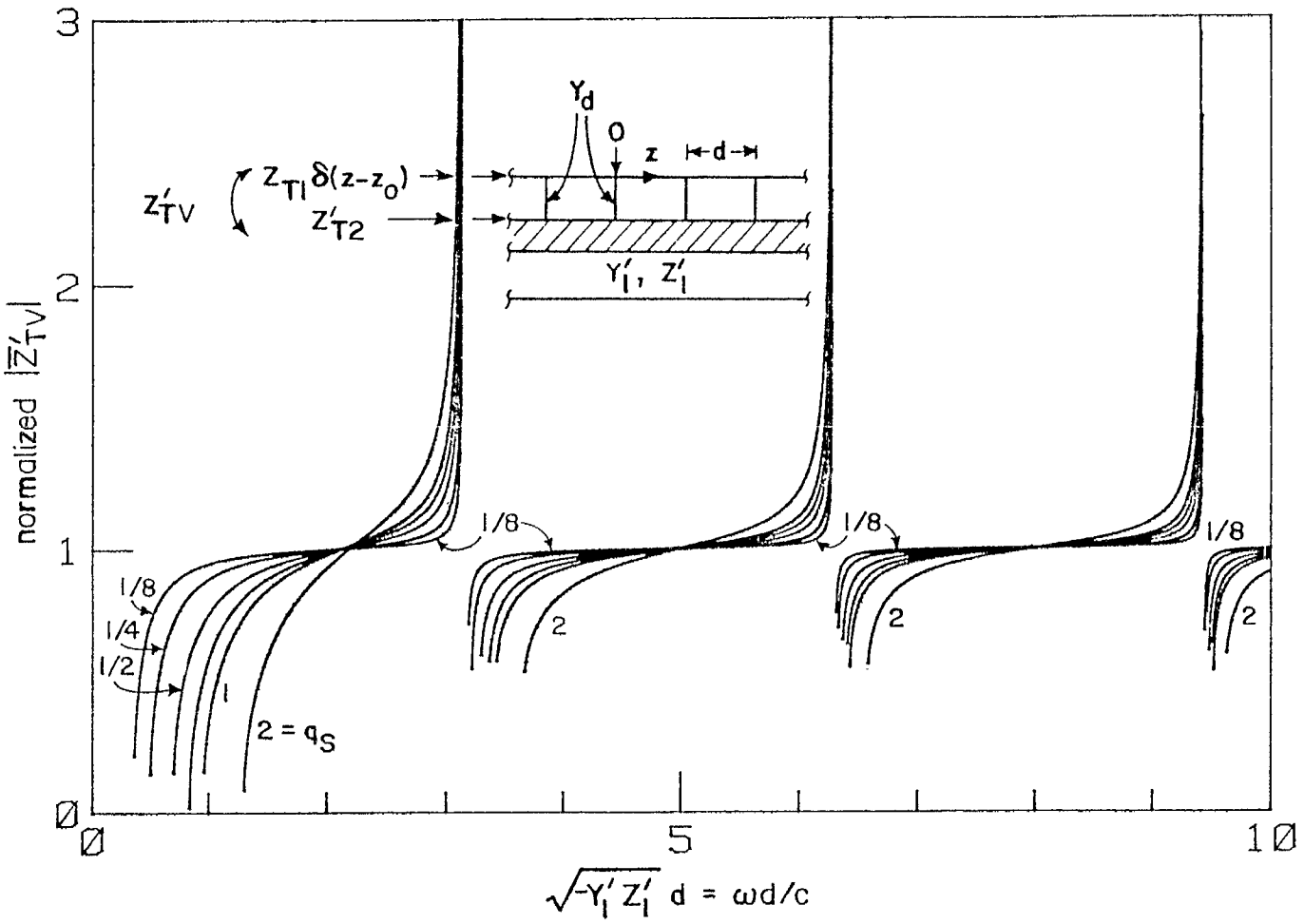

Figure 8. Normalized $|\overline{Z}'_{TV}|$ (normalized to their values when the cable shields are not bonded) when $z_o = 0$ versus frequencies for various $q_S = Z'_1 Y_d d$.

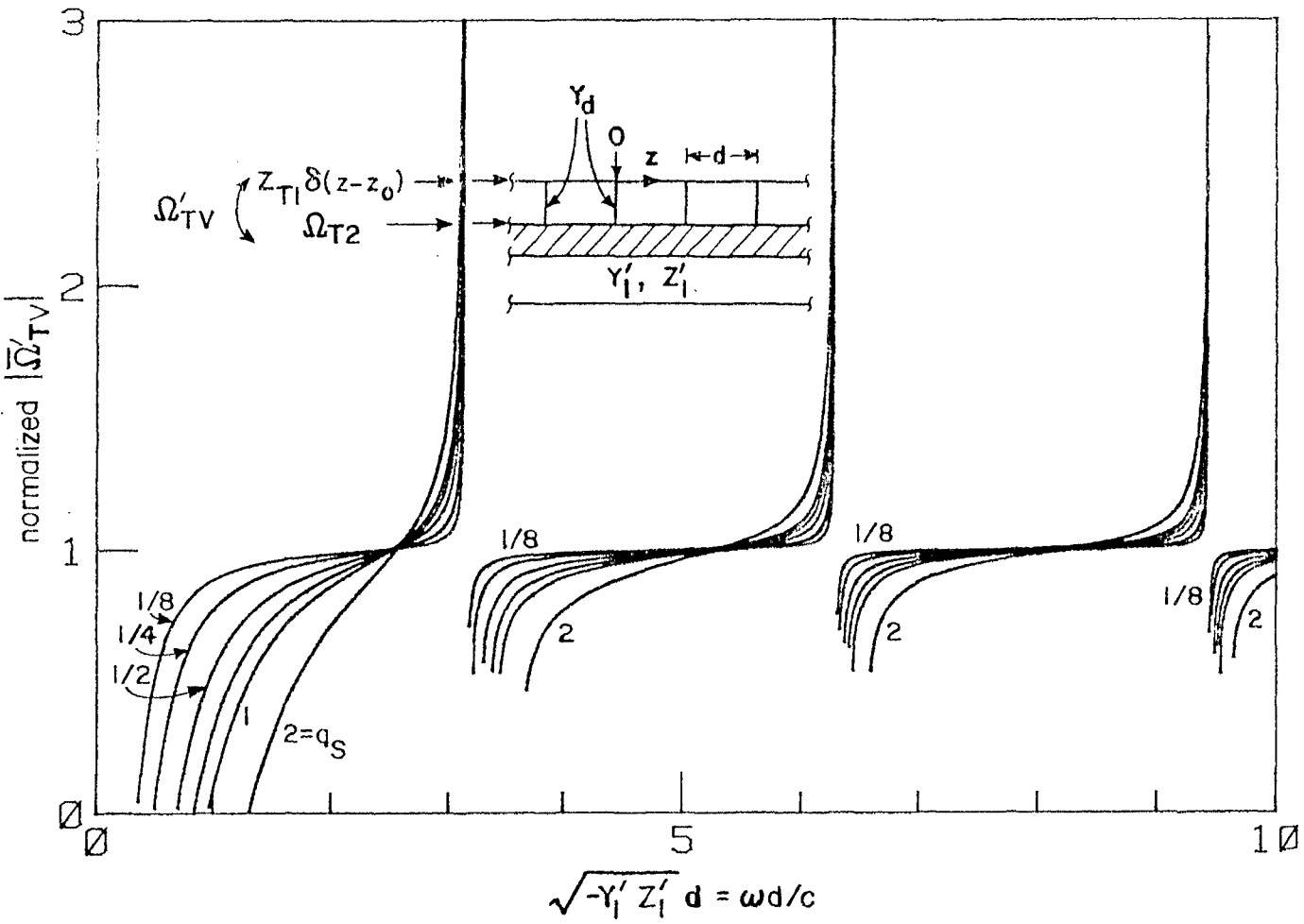

Figure 9. Normalized $|\bar{\Omega}'_{TV}|$ when $z_o = 0$ versus frequencies for various $q_S = Z'_1 Y_d d$.

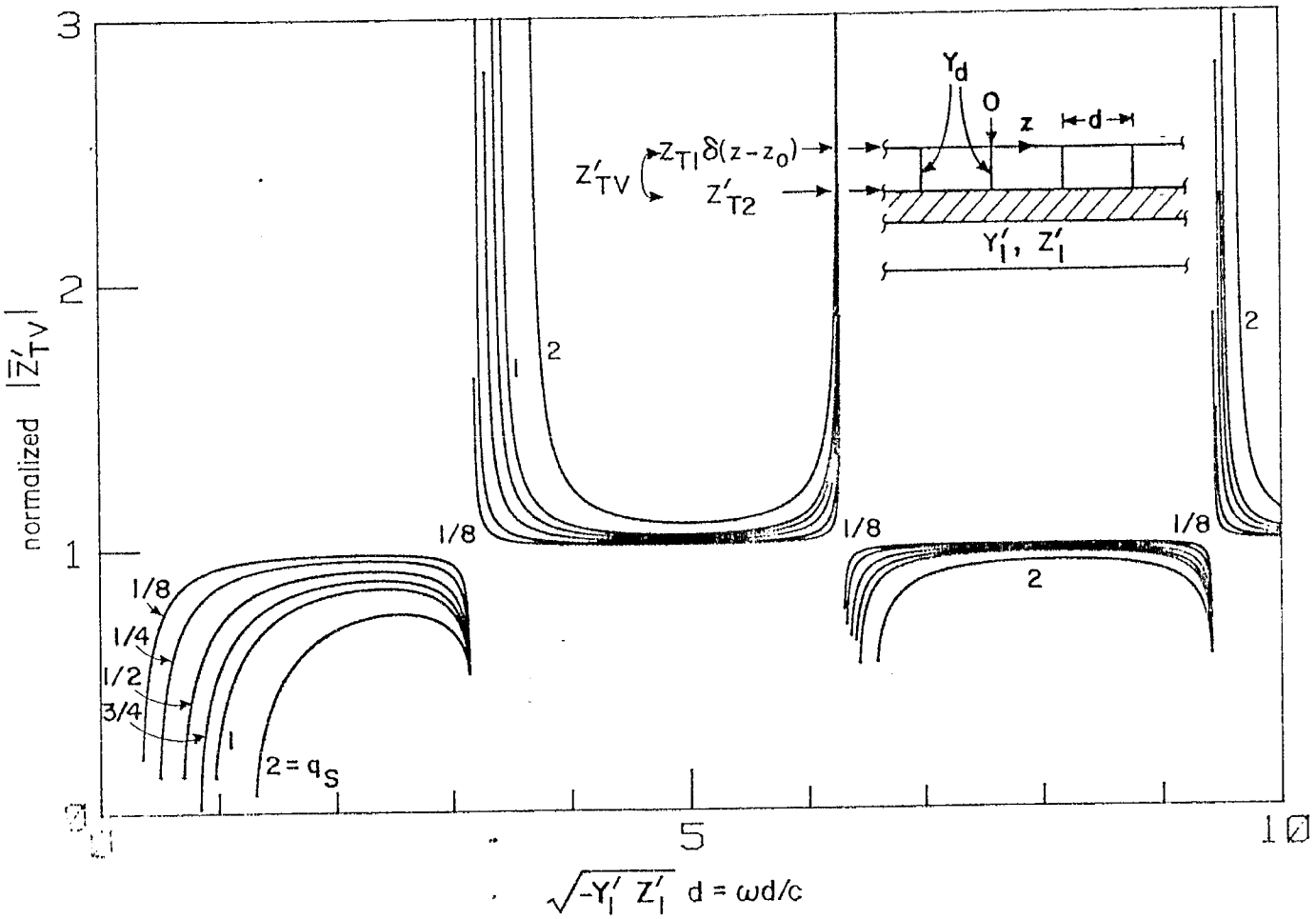

Figure 10. Normalized $|\bar{Z}'_{TV}|$ when $z_o = d/2$ versus frequencies for various $q_S = Z'_1 Y_d d$.

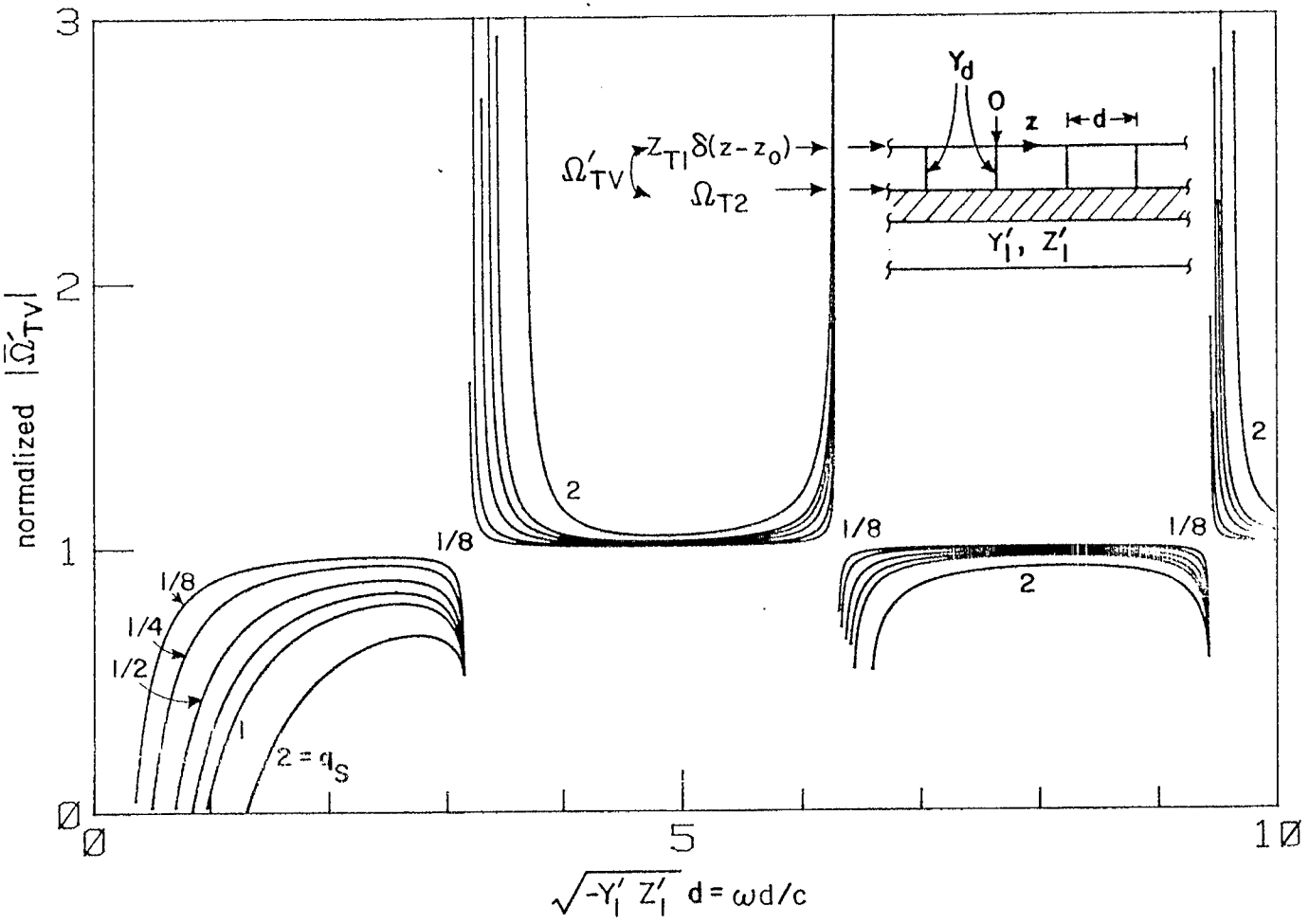

Figure 11. Normalized $|\bar{\Omega}'_{TV}|$ when $z_o = d/2$ versus frequencies for various $q_S = Z'_1 Y_d d$.

The voltage, current and charge distributions of the double shield due to the current source shown in Figure 5 can then be completely described by Equations 8, 11, 12 13 and 22, provided that I^s is known. Here, similar to the voltage-source case, for the problem of Figure 3b, I^s is I^s_o. To obtain I^s ($I^s = I^s_1$ for $z > z_o$, $I^s = I^s_2$ for $z < z_o$) for the problem of Figure 3a or 4b, one has to solve Equations 11, 12 and the equations given in Figure 4b. For the special cases of $z_o = 0$ and $d/2$, $I^s = I^s_1 = I^s_2 = I^s_o/2$. From these current and charge distributions, one can calculate the voltage- and current-source terms of the transmission-line equations of the inside cables using Equations 16 and 17.

The current source of the shield I^s_o can generally be estimated from the short-circuit charge density Q'_{sc} on the outermost surface of the double shield and the localized charge transfer frequency Ω^L_{T1} (which has a dimension of frequency × length, different from that of Ω_{T2}) of the outer shield via (for example, see Equation 38 of Reference 5)

$$I^s_o = Q'_{sc}\Omega^L_{T1} \tag{23}$$

One can also define an effective transfer impedance Z_{TI} and an effective charge transfer frequency for the double shield as follows:

$$Z_{TI}(z) = V'_s(z)/(j\omega Q'_{sc}) \tag{24}$$

$$\Omega_{TI}(z) = I'_s(z)/Q'_{sc} \tag{25}$$

where the subscript "I" is used to indicate that the quantities are for a localized "current" source which is generated by Q'_{sc}.

Similar to Z'_{TV} and Ω_{TV} of the voltage-source case, Z_{TI} and Ω_{TI} are also z-dependent. They become very small far away from z_o in the stopbands, are oscillatory and modulated by the periodicity of the straps in the passbands. The averaged quantities $\overline{Z}_{TI}$ and $\overline{\Omega}_{TI}$ are given by

$$\bar{Z}_{TI} \Big/ \left(\frac{\Omega_{T1}^{L} Z'_{T2}}{n_p j\omega} \right) = \frac{\sqrt{-Z'_1 Y'_1}\, d}{kd} \cdot \bar{\Omega}_{TI} \Big/ \left(\frac{\Omega_{T1}^{L} \Omega_{T2} \sqrt{-Z'_1 Y'_1}\, d}{n_p \omega d} \right)$$

$$= \frac{-(Z'_1 Y_d d)(kd)\exp(jkd/2)}{\sqrt{-Z'_1 Y'_1}\, d\, (k^2 + Y'_1 Z'_1) d^2} \times$$

$$\times \left\{ \frac{\sin(kd/2)\cos[(z_o - d/2)\sqrt{-Z'_1 Y'_1}]}{\sin(d\sqrt{-Z'_1 Y'_1}/2)} \right.$$

$$\left. - j \frac{\cos(kd/2)\sin[(z_o - d/2)\sqrt{-Z'_1 Y'_1}]}{\cos(d\sqrt{-Z'_1 Y'_1}/2)} \right\}^{-1} \qquad (26)$$

$\bar{Z}_{TI}$ and $\bar{\Omega}_{TI}$ also depend on where $z = z_o$ is. However, no matter where z_o is, one still sees that the normalized $|\bar{Z}_{TI}|$ and $|\bar{\Omega}_{TI}|$ (normalized with respect to their values when there is no bonding, which are, respectively, $\Omega_{T1}^{L} Z'_{T2}/(j\omega n_p)$ and $\Omega_{T1}^{L} \Omega_{T2} \sqrt{-Z'_1 Y'_1}/(n_p \omega)$) are greater than unity for some $\sqrt{-Z'_1 Y'_1}\, d$ (where the bondings degrade the shielding effectiveness) and smaller than unity for the others. Examples of the normalized $|\bar{Z}_{TI}|$ and $|\bar{\Omega}_{TI}|$ for $z_o = d/2$ as functions of $\sqrt{-Z'_1 Y'_1}\, d$ and q_s are plotted in Figures 12 and 13. Similar to Figures 8 through 11, the values at the stopbands are not given. For better shielding effectiveness, one should try to increase $Z'_1 Y_d$ and avoid $\omega d/c \simeq n\pi$ $(n = 1,2,3, \ldots)$.

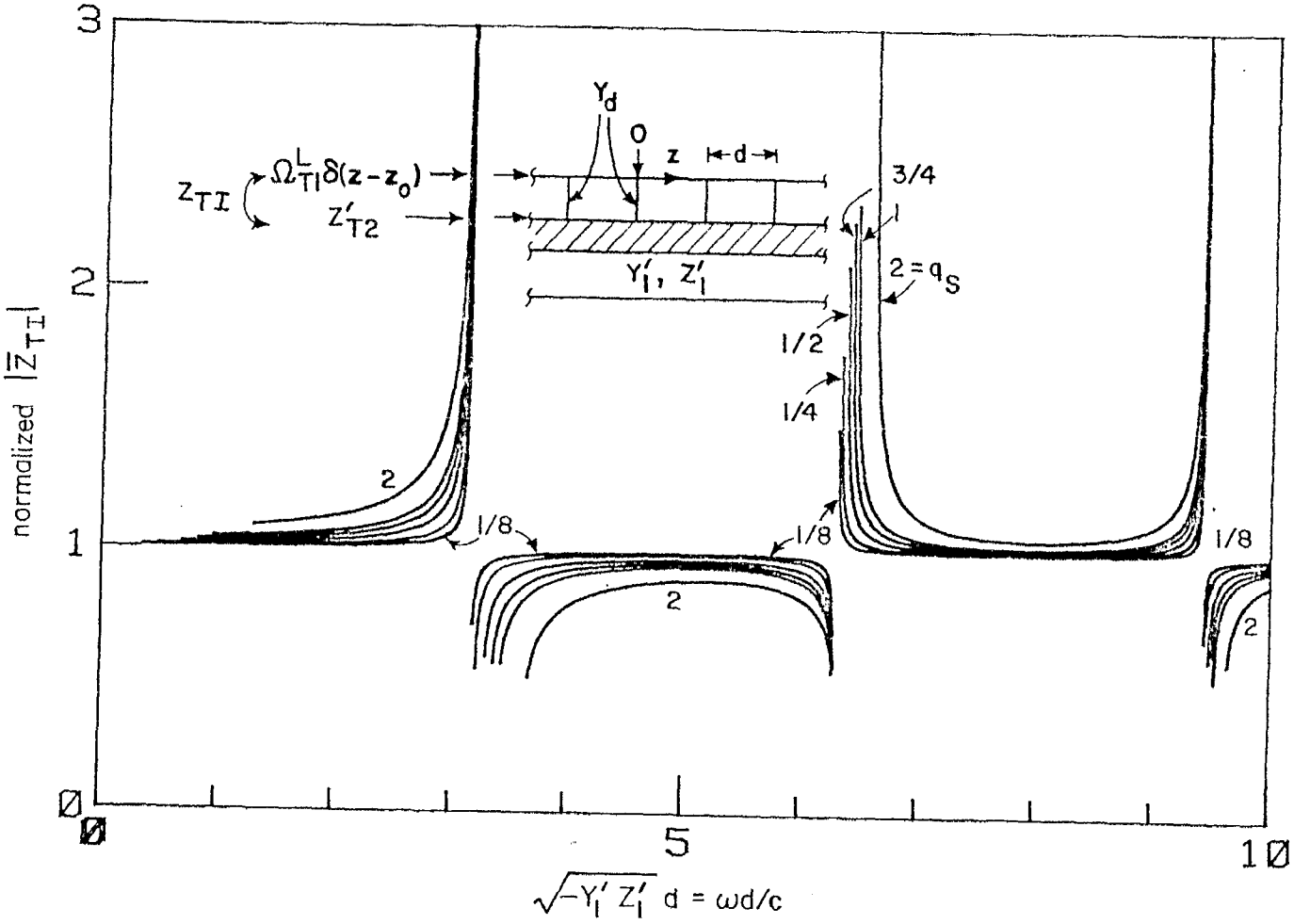

Figure 12. Normalized $|\overline{Z}_{TI}|$ when $z_o = d/2$ versus frequencies for various $q_S = Z_1' Y_d d$.

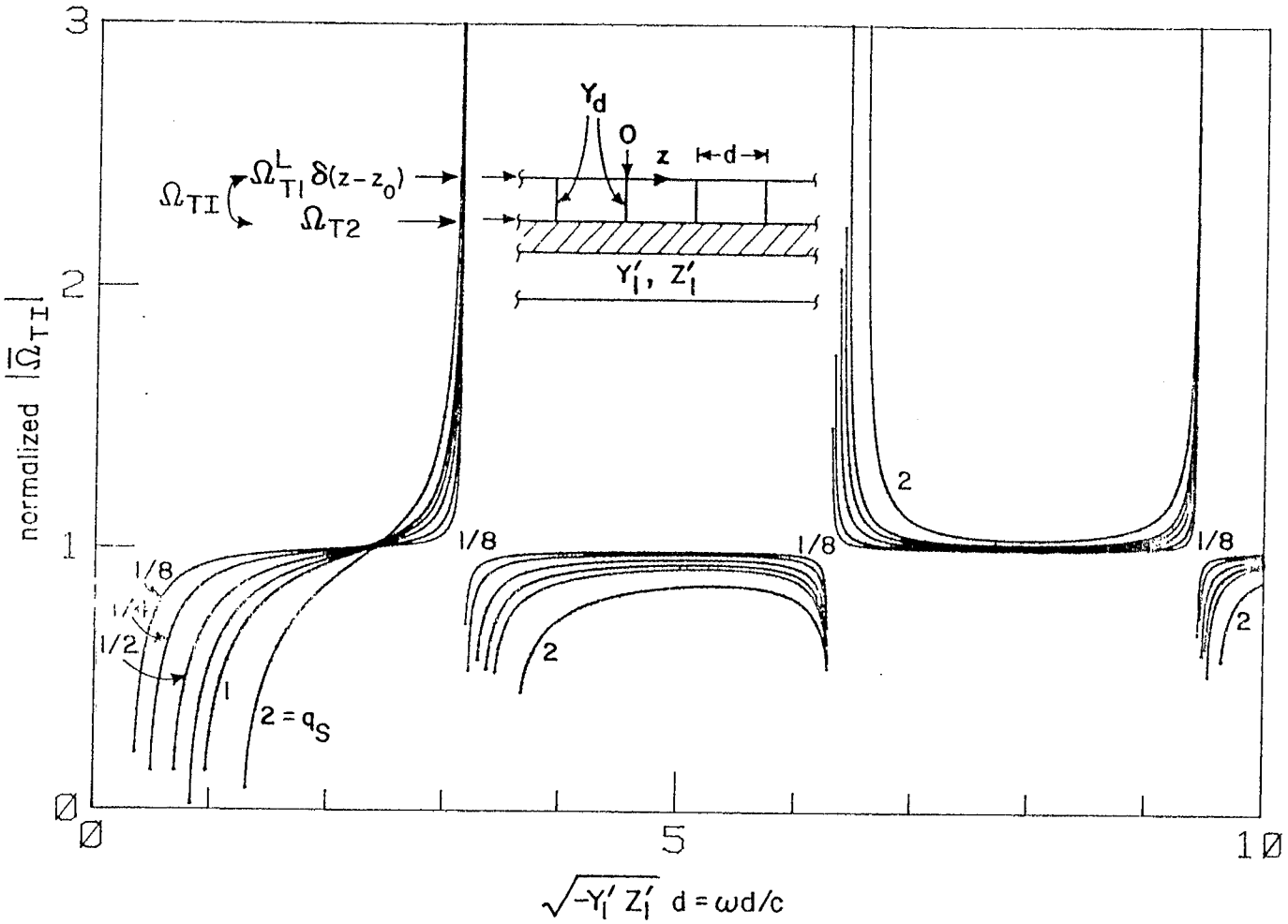

Figure 13. Normalized $|\overline{\Omega}_{TI}|$ when $z_o = d/2$ versus frequencies for various $q_S = Z_1' Y_d d$.

III. DISTRIBUTED EXCITATIONS

In this section both the outer and inner shields are assumed to have uniformly distributed transfer functions: Z'_{T1} (shield transfer impedance per unit length), Ω_{T1} (charge transfer frequency) for the outer shield and Z'_{T2}, Ω_{T2} for the inner shield (Figs. 2 and 14). The outer shield is different from that discussed in Section II which has localized transfer parameters. The total current I_t and total charge per unit length Q'_t of the double-shield cable are assumed known. I_t and Q'_t are also assumed to be dependent upon z as exp(-jhz) and related to each other via

$$j\omega Q'_t = -\frac{d}{dz} I_t = jhI_t \tag{27}$$

In what follows, results for this distributed double shield without bonding straps are presented first, and then, the more general case with periodic bonding straps is discussed.

1. SCHELKUNOFF'S CIRCUIT (REF. 6)

When the shields are solid tubular conductors, $\Omega_{T1} = \Omega_{T2} = 0$, and the current-source term I'_s of the transmission-line equations of the inside cables vanishes. As for the voltage-source term V'_s, when $hd \approx 0$ and $\omega\mu_i\sigma_i >> h^2$, it can be calculated from the circuit depicted in Figure 15 which is valid regardless whether the bondings are present or not (see Ref. 6). The circuit elements in the figure are defined and given as follows:

Z'_{ai} = surface impedance per unit length of the i-th shield with internal return (i = 1 for the outer shield, i = 2 for the inner shield)

$$= \frac{\gamma_i}{2\pi a_i \sigma_i D_i}\left[I_o(\gamma_i a_i)K_1(\gamma_i b_i) + K_o(\gamma_i a_i)I_1(\gamma_i b_i)\right]$$

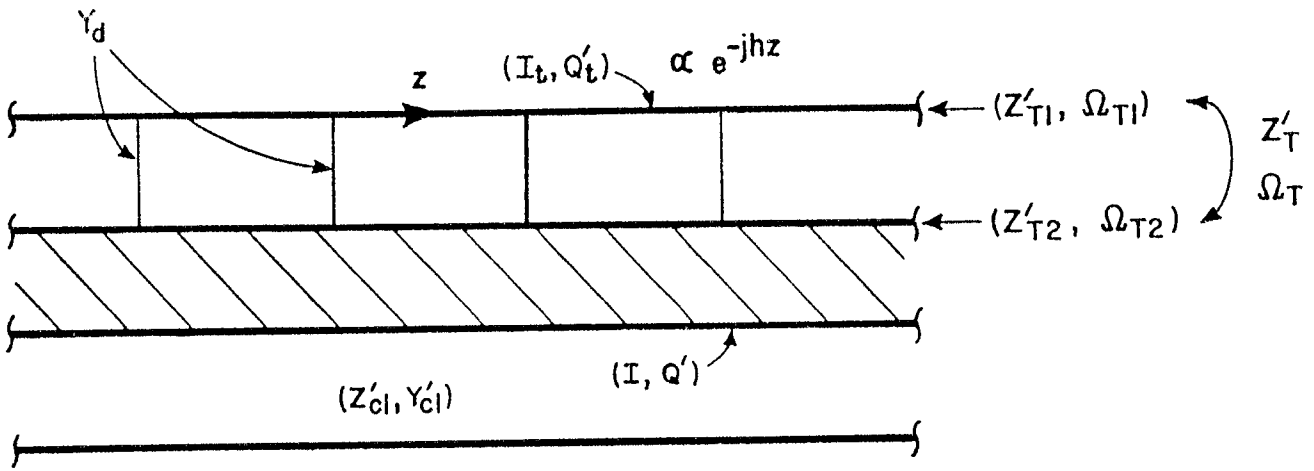

Figure 14. A theoretical model for a distributed excited double shield with periodic bondings.

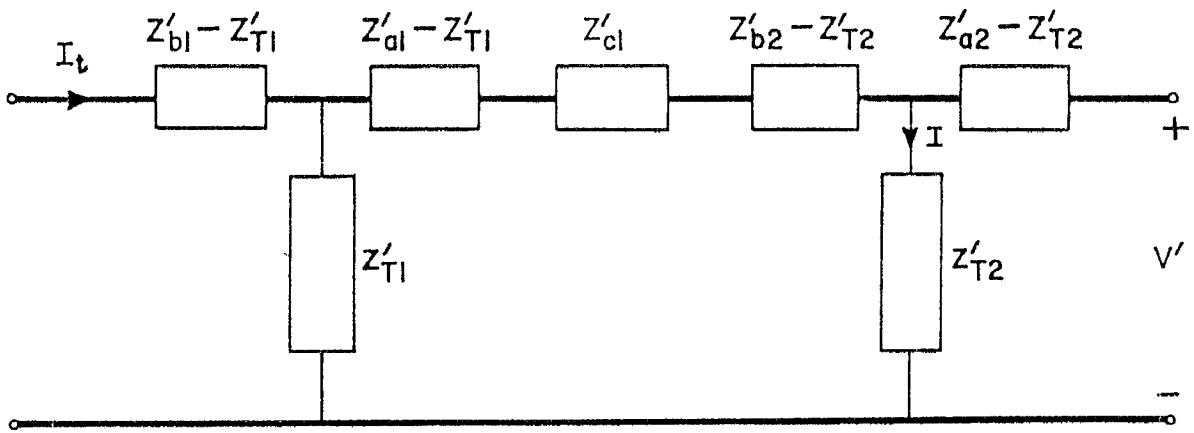

$$\frac{Z'_T}{Z'_{T2}} = \frac{I}{I_t}$$

Figure 15. Schelkunoff's circuit for the calculation of Z'_T of a solid tubular double shield with or without periodic bondings.

Z'_{bi} = surface impedance per unit length of the i-th shield with external return

$$= \frac{\gamma_i}{2\pi b_i \sigma_i D_i}\left[I_o(\gamma_i b_i)K_1(\gamma_i a_i) + K_o(\gamma_i b_i)I_1(\gamma_i a_i)\right] \tag{28}$$

$$Z'_{Ti} = \frac{1}{2\pi\sigma_i a_i b_i D_i}$$

Z'_{c1} = series impedance per unit length of the double shield when assumed perfect

$$= j\omega\mu_o \ell n(a_1/b_2)/(2\pi)$$

where

$$D_i = I_1(\gamma_i b_i)K_1(\gamma_i a_i) - I_1(\gamma_i a_i)K_1(\gamma_i b_i)$$

$$\gamma_i^2 \simeq j\omega\mu_i\sigma_i = 2j/\delta_i^2 \tag{29}$$

μ_i, σ_i, a_i, b_i, δ_i = permeability, conductivity, inner radius, outer radius, skin depth of the i-th shield

and I_o, I_1, K_o, K_1 are the modified Bessel functions. From the circuit, one immediately finds that the effective transfer impedance per unit length Z'_T ($= V'_s/I_t$) of the double shield is given by

$$Z'_T = \frac{Z'_{T1}Z'_{T2}}{Z'_{a1} + Z'_{b2} + Z'_{c1}} = \frac{Z'_{T1}Z'_{T2}}{Z'_1} \tag{30}$$

where

$$Z'_1 = Z'_{a1} + Z'_{b2} + Z'_{c1} \tag{31}$$

Evidently, Equation 30 and the circuit in Figure 15 can be extended easily to describe the effective transfer impedance per unit length of a N-surface solid tubular shield with N > 2.

Although Equation 30 looks simple, the circuit elements in the expression are complicated functions of frequency and shield parameters (see Eqs. 28 and 29). When Δ_i (= $b_i - a_i$, the thickness of the i-th shield) << a_i, b_i and $\gamma_i a_i$, $\gamma_i b_i$ >> 1, the circuit elements Z'_{bi}, Z'_{ai}, Z'_{Ti} can be approximated by

$$Z'_{ai} \simeq Z'_{bi} \simeq Z'_{Ii} = \frac{\gamma_i \Delta_i}{2\pi\sqrt{a_i b_i}\sigma_i \Delta_i} \coth(\gamma_i \Delta_i) \tag{32}$$

$$Z'_{Ti} \simeq \frac{\gamma_i \Delta_i}{2\pi\sqrt{a_i b_i}\sigma_i \Delta_i} \operatorname{csch}(\gamma_i \Delta_i) \tag{33}$$

where Z'_{Ii} is referred to as the internal impedance per unit length of the i-th shield. Equations 32 and 33 can be further approximated by

$$Z'_{ai} \simeq Z'_{bi} \simeq Z'_{Ii} \simeq Z'_{Ti} \simeq R'_{dc,i} = \frac{1}{2\pi\sqrt{a_i b_i}\sigma_i \Delta_i} \tag{34}$$

when $\gamma_i \Delta_i$ << 1 (i.e., δ_i >> Δ_i), and

$$Z'_{ai} \simeq Z'_{bi} \simeq Z'_{Ii} \simeq \gamma_i \Delta_i R'_{dc,i} \tag{35}$$

$$Z'_{Ti} \simeq 2\gamma_i \Delta_i R'_{dc,i} e^{-\gamma_i \Delta_i} \tag{36}$$

when $\gamma_i \Delta_i$ >> 1 (i.e., Δ_i >> δ_i). Here, $R'_{dc,i}$ is the dc-shield resistance per unit length of the i-th shield and the real part of γ_i is taken to be positive.

2. CASEY'S CIRCUIT (REF. 7)

When δ_i >> Δ_i (which guarantees $Z'_{ai} \simeq Z'_{bi} \simeq Z'_{Ii} \simeq Z'_{Ti}$, see Eq. 34), $h^2 b_1^2 \simeq - Z'_1 Y'_1 b_1^2 \simeq - Z'_{c1} Y'_{c1} b_1^{'2}$ << 1 (Y'_{c1} is the shunt admittance per unit length of the double shield when assumed perfect and no bonding straps), and there is no bonding strap, the circuit diagram shown in Figure 16 can be used to calculate the current I flowing on the inner shield (Ref. 7). In the

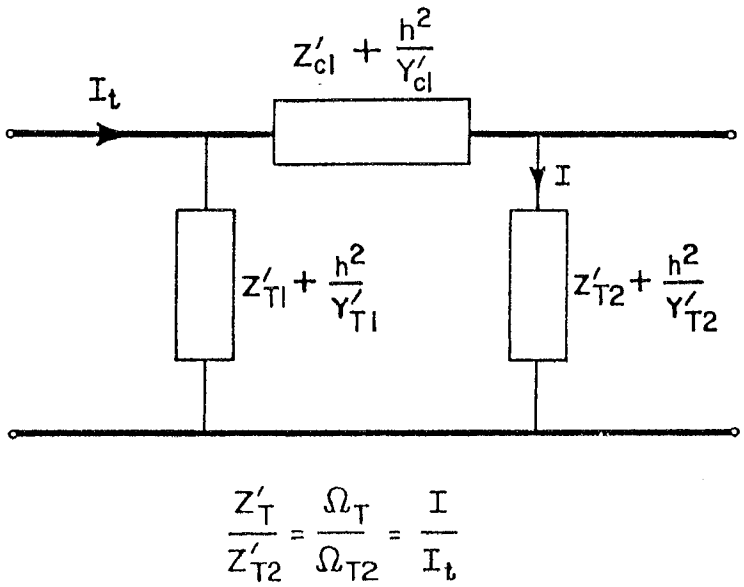

Figure 16. Casey's circuit for the calculations of Z'_T and Ω_T of a double shield without periodic bonding.

circuit Y'_{Ti} $(i = 1,2)$ are the capacitive transfer admittances per unit length of the shields, which are related to Ω_{Ti} via,

$$\Omega_{Ti} = - sY'_i/Y'_{Ti} \tag{37}$$

where

$$\frac{1}{Y'_1} = \frac{1}{Y'_{c1}} + \frac{1}{Y'_{T1}} + \frac{1}{Y'_{T2}} \tag{38}$$

$$\frac{1}{Y'_2} = \frac{1}{Y'_{c2}} + \frac{1}{Y'_{T2}} \tag{39}$$

and Y'_{c2} is the shunt admittance per unit length of transmission line formed by the inner shield and the wires within when $Y'_{T2} = \infty$.

From the circuit, one has

$$\frac{I}{I_t} = \frac{Z'_{T1} + h^2/Y'_{T1}}{(Z'_{T1} + h^2/Y'_{T1}) + (Z'_{T2} + h^2/Y'_{T2}) + (Z'_{c1} + h^2/Y'_{c1})}$$

$$= \frac{Z'_{T1} + h^2/Y'_{T1}}{Z'_1 + h^2/Y'_1} \tag{40}$$

where

$$Z'_1 = Z'_{T1} + Z'_{T2} + Z'_{c1} \tag{41}$$

from which one immediately has

$$\frac{Z'_T}{Z'_{T2}} = \frac{\Omega_T}{\Omega_{T2}} = \frac{Z'_{T1} + h^2/Y'_{T1}}{Z'_1 + h^2/Y'_1} \tag{42}$$

When $h \to 0$ and $Y'_{T1} = Y'_{T2} = \infty$, Equation 42, indeed, reduces to Equation 30 with $\delta_i >> \Delta_i$. It is believed that the above thin shield $(\delta_i >> \Delta_i)$

approximation, Equation 42, can also be used for thick shields provided that Z_1' defined in Equation 41 is replaced by Equation 31, i.e.,

$$Z_1' = Z_{a1}' + Z_{b2}' + Z_{c1}'$$

and a more general circuit can be constructed (see Fig. 17). Here, the circuit elements Z_{a1}' and Z_{b2}' should be defined in a broader sense than Equation 28 to include all kinds of penetrations. This circuit can also be easily extended to describe a N-surface shield with N > 2.

Up to this point the discussion in Part 2 has been restricted to the situation that there is no bonding connecting the shields. When there are periodic bondings with period $d << h^{-1}$, $(\sqrt{-Y_1'Z_1'})^{-1}$, it is postulated that the circuits and equations can still be used provided that Y_1' is replaced by $Y_1' + Y_d/d$, i.e., Equation 42 becomes

$$\frac{Z_T'}{Z_{T2}'} = \frac{\Omega_T}{\Omega_{T2}} = \frac{Z_{T1}' + h^2/Y_{T1}'}{Z_1' + h^2/(Y_1' + Y_d/d)} \qquad (43)$$

In the following, a general analysis of a double shield with periodic bondings will be given. The results of the analysis will show whether the simple Equation 43 is accurate enough under the imposed conditions.

3. GENERAL FORMULATION

To obtain the current I flowing on the inner shield one has to solve the following transmission-line equations (Fig. 14):

$$\frac{dV}{dz} + Z_1'I = Z_{T1}'I_t \qquad (44)$$

$$\frac{dI}{dz} + \left[Y_1' + Y_d \sum_{n=-\infty}^{\infty} \delta(z - nd) \right] V = - j\omega \frac{Y_1'}{Y_{T1}'} Q_t' \qquad (45)$$

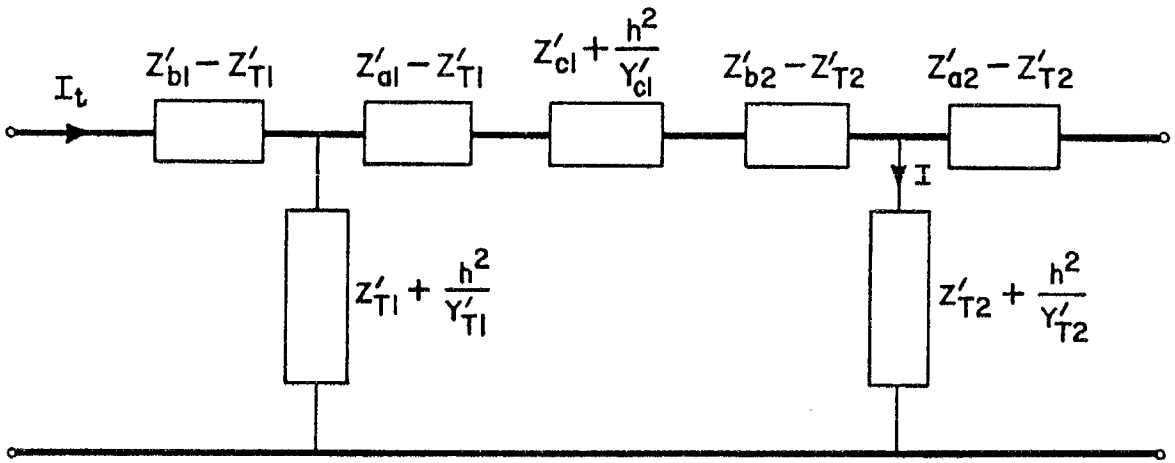

Figure 17. Generalized Casey's circuit (constraints $\delta_i >> \Delta_i$ in Casey's circuit are lifted) for the calculations of Z'_T and Ω_T of a double shield without periodic bonding.

The shields are assumed to be infinitely extended in both +z and -z directions so that only the particular solution of the equations need be considered. This particular solution can be written as follows (from Floquet's theorem)

$$I(z) = e^{-jhz} \sum_{n=-\infty}^{\infty} I_n^p e^{-j2n\pi z/d} \tag{46}$$

$$V(z) = e^{-jhz} \sum_{n=-\infty}^{\infty} V_n^p e^{-j2n\pi z/d} \tag{47}$$

After substituting Equations 46 and 47 into Equations 44 and 45, and going through some complicated algebraic manipulations and series summations, one eventually has, for $md \leq z < (m+1)d$,

$$I(z) = I_t \frac{Y_1'}{Y_{T1}'} \frac{h^2 + Z_{T1}' Y_{T1}'}{h^2 + Z_1' Y_1'} \left\{ 1 + \frac{hY_d}{2Y_1'} \frac{Z_{T1}' Y_{T1}' - Z_1' Y_1'}{Z_{T1}' Y_{T1}' + h^2} \times \right.$$

$$\left. \times \sum_{n=1}^{2} \frac{\sin[(h+(-1)^n\sqrt{-Y_1'Z_1'})d/2]\exp[-j(h-(-1)^n\sqrt{-Y_1'Z_1'})(md - z + d/2)]}{\cos(d\sqrt{-Y_1'Z_1'}) - \cos(hd) + Y_d Z_1' \sin(d\sqrt{-Y_1'Z_1'})/(2\sqrt{-Y_1'Z_1'})} \right\} \tag{48}$$

from which $Q'(z)$, Z_T' and Ω_T can be calculated via

$$Q'(z) = -\frac{1}{j\omega} \frac{d}{dz} I(z) \tag{49}$$

$$Z_T' = Z_{T2}' I(z)/I_t \tag{50}$$

$$\Omega_T = \frac{j\Omega_{T2}}{h} \frac{d}{dz} \frac{I(z)}{I_t} \tag{51}$$

Both Z_T' and Ω_T are z-dependent. In order to better quantify the transfer functions, one takes the average values of Z_T' and Ω_T over the period d of the bonding straps. These average values, designated as $\overline{Z}_T'$ and $\overline{\Omega}_T$, are independent of z and are given as

$$\frac{\overline{Z}'_T}{Z'_{T2}} = \frac{\overline{\Omega}_T}{\Omega_{T2}} = \frac{I_o P_e^{-jhz}}{I_t}$$

$$= \frac{Y'_1}{Y'_{T1}} \frac{h^2 + Z'_{T1}Y'_{T1}}{h^2 + Z'_1 Y'_1} \left\{ 1 + \frac{h^2}{h^2 + Z'_1 Y'_1} \frac{Z'_{T1}Y'_{T1} - Z'_1 Y'_1}{Z'_{T1}Y'_{T1} + h^2} \times \right.$$

$$\left. \times \frac{Y_d}{dY'_1} \frac{\cos(d\sqrt{-Y'_1 Z'_1}) - \cos(hd)}{\cos(d\sqrt{-Y'_1 Z'_1}) - \cos(hd) + Y_d Z'_1 \sin(d\sqrt{-Y'_1 Z'_1})/(2\sqrt{-Y'_1 Z'_1})} \right\} \qquad (52)$$

It can be shown that Equation 52 reduces to Equation 43 when

$$\left| hd - \sqrt{-Y'_1 Z'_1}\, d \right| = |\alpha| << 1, \qquad hd >> q_S \ (= Z'_{c1} Y_d d) \qquad (53)$$

$$|\tan hd| >> |\alpha|, \quad (\text{i.e., } |hd - n\pi| >> |\alpha|, \ n = 0,1,2, \ldots) \qquad (54)$$

The conditions 53 and 54, obviously, are different and less restrictive than those imposed on Equation 43 during the discussion in Part 2. In most practical situations, Conditions 53 and 54 can be satisfied, and Equation 43 can be used. In the case that the constraints 53 and 54 are not met, one has to resort to Equation 52 which is a complicated function of the frequency and the shield parameters. The shield parameters Z'_{T1}, Y'_{T1}, Y'_1, Z'_1, etc., are generally complex values. However, when the diffusion penetration is not important (which is true for most highly conducting shields at frequencies larger than 10 kHz), the shield parameters Z'_{T1}, Y'_{T1}, etc., become purely imaginary (i.e., the penetration is through the apertures such as in the case of braided cable shields), and Equation 52 becomes a real function. This real function is plotted in Figures 18 through 25 as a function of $hd \simeq \sqrt{-Y'_{c1}Z'_{c1}}\, d = \omega d/c$ (from 0 to 10) by using $q_Z = Z'_{T1}/Z'_{c1}$, $q_Y = Y'_{c1}/Y'_{T1}$ and $q_S = Z'_{c1}Y_d d$ (= 0.1, 0.5, 1,2) as parameters (also assume $Z'_{T2}/Z'_{c1} \simeq 0$, $Y'_{c1}/Y'_{T2} \simeq 0$). The values for the parameters (q_Y, q_Z) = (0.004, 0.01) and (0.001, 0.002) are for some typical braided cable shields (see

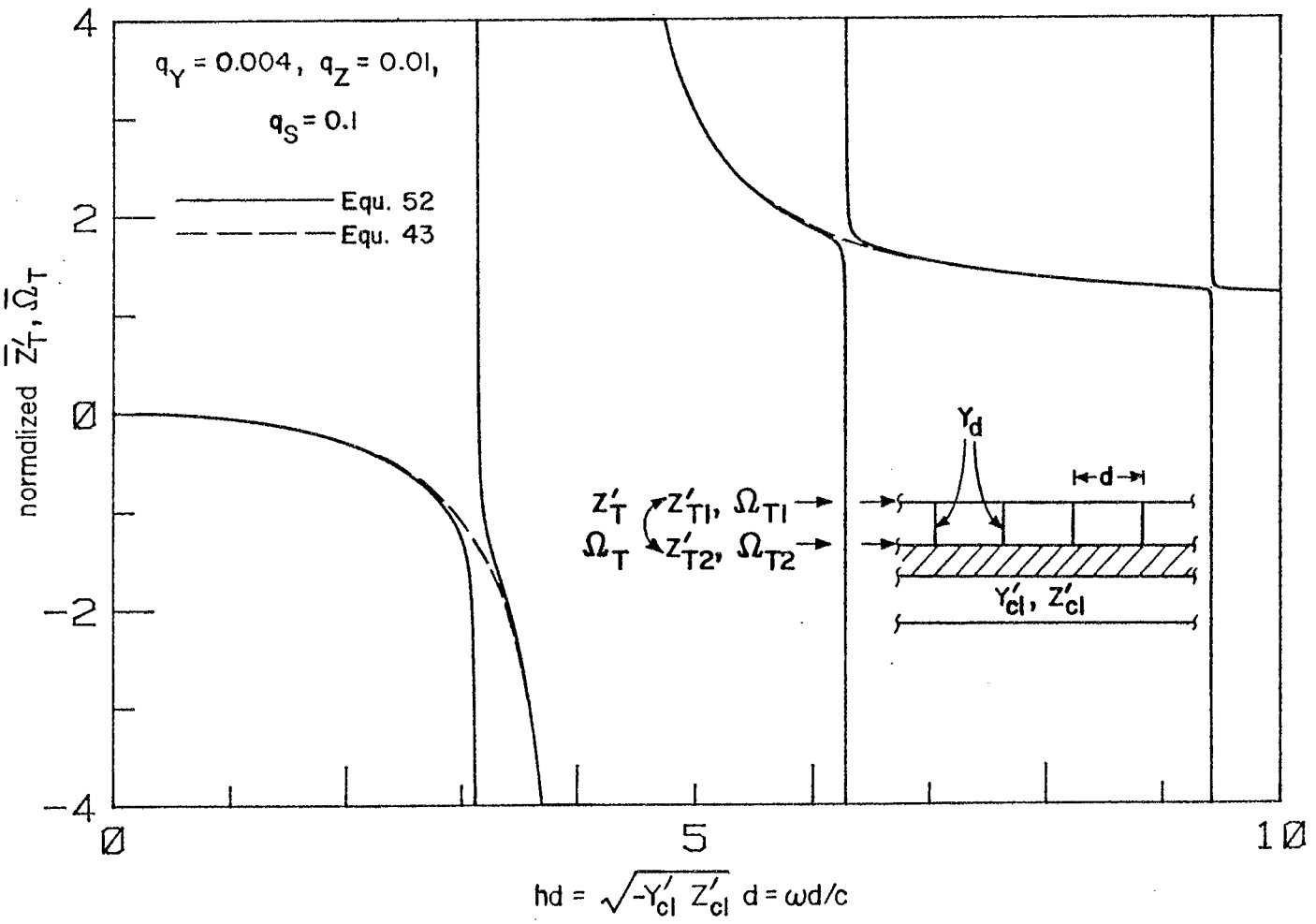

Figure 18. Normalized $\bar{Z}'_T$ and $\bar{\Omega}_T$ (normalized to their values when the cable shields are not bonded), based on the general Equation 52 and the approximated Equation 43, versus frequencies for $q_S = Z'_{c1} Y_d d = 0.1$, $q_Y = Y'_{c1}/Y'_{T1} = 0.004$ and $q_Z = Z'_{T1}/Z'_{c1} = 0.01$.

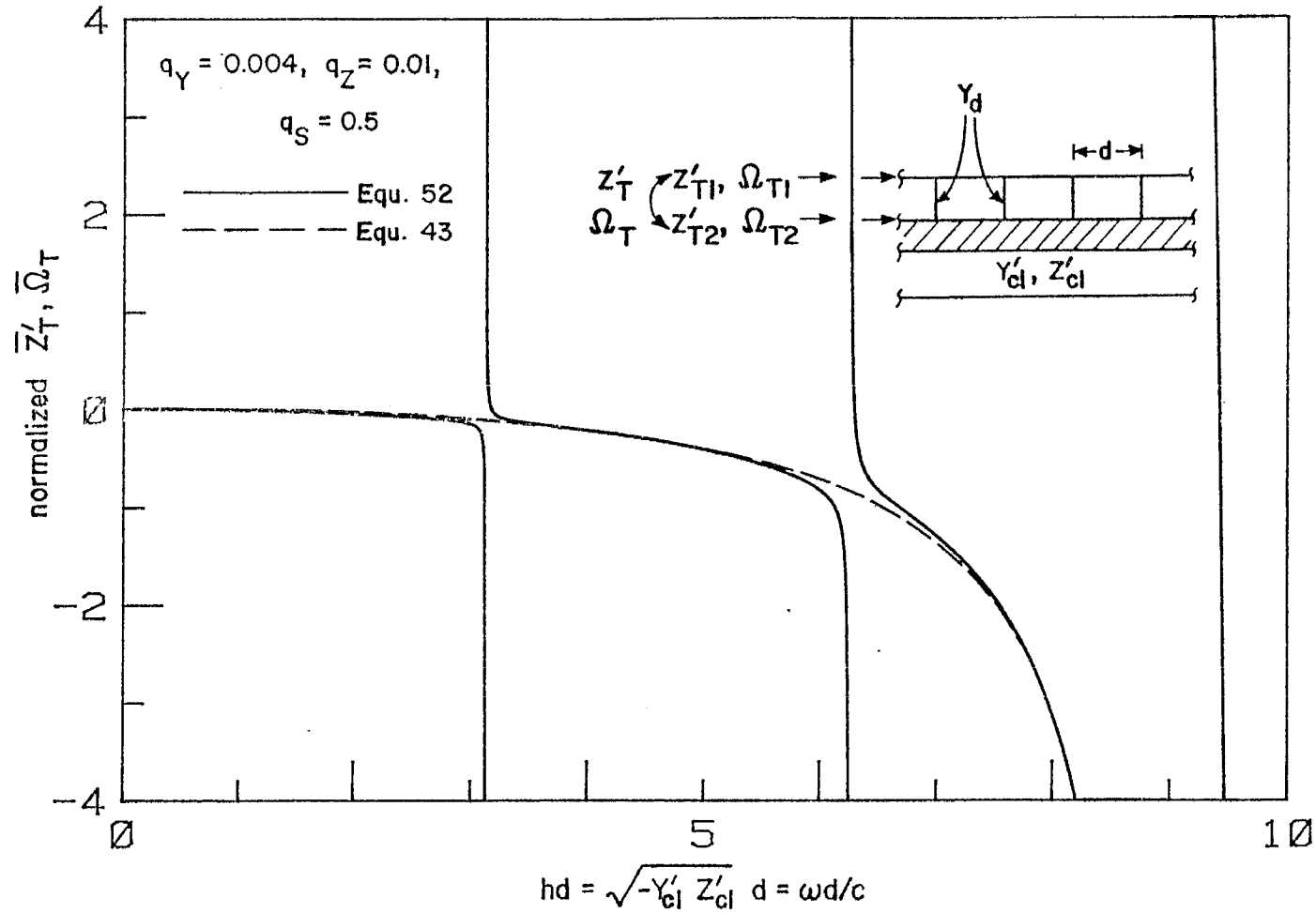

Figure 19. Normalized $\overline{Z}'_T$ and $\overline{\Omega}_T$ (normalized to their values when the cable shields are not bonded), based on the general Equation 52 and the approximated Equation 43, versus frequencies for $q_S = Z'_{c1} Y_d d = 0.5$, $q_Y = Y'_{c1}/Y'_{T1} = 0.004$ and $q_Z = Z'_{T1}/Z'_{c1} = 0.01$.

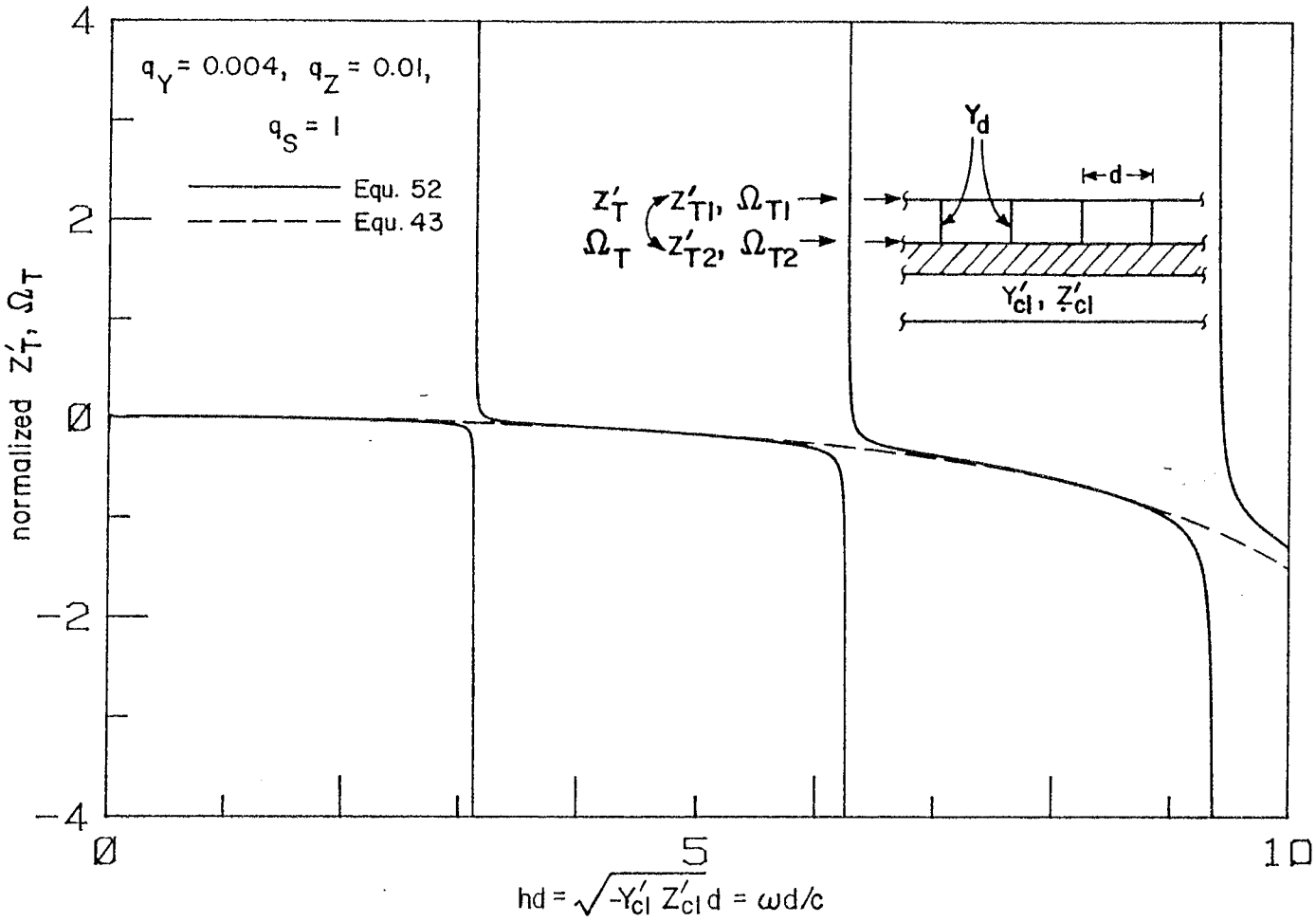

Figure 20. Normalized $\bar{Z}'_T$ and $\bar{\Omega}_T$ (normalized to their values when the cable shields are not bonded), based on the general Equation 52 and the approximated Equation 43, versus frequencies for $q_S = Z'_{c1} Y_d d = 1$, $q_Y = Y'_{c1}/Y'_{T1} = 0.004$ and $q_Z = Z'_{T1}/Z'_{c1} = 0.01$.

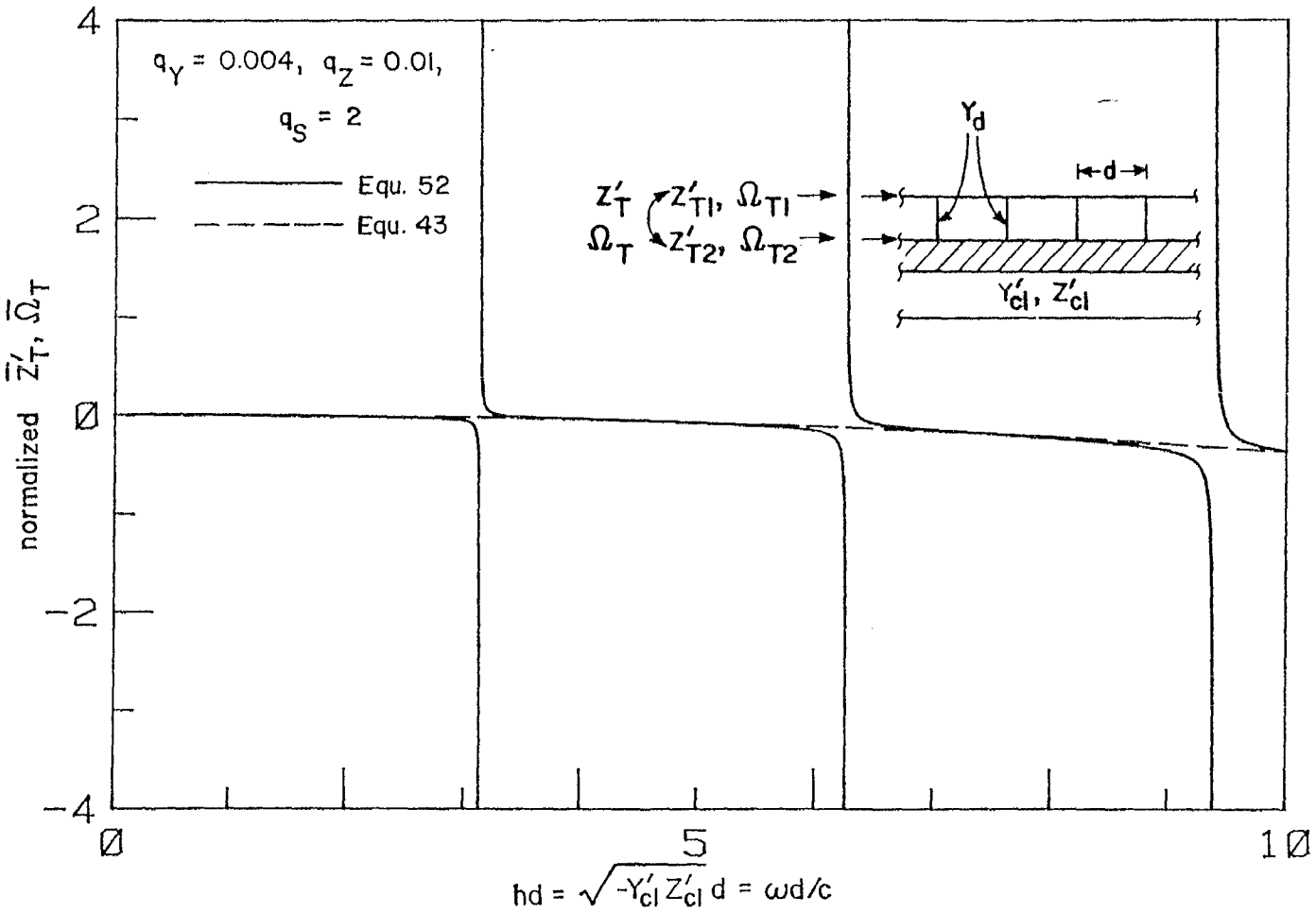

Figure 21. Normalized $\bar{Z}'_T$ and $\bar{\Omega}_T$ (normalized to their values when the cable shields are not bonded), based on the general Equation 52 and the approximated Equation 43, versus frequencies for $q_S = Z'_{c1} Y_d d = 2$, $q_Y = Y'_{c1}/Y'_{T1} = 0.004$ and $q_Z = Z'_{T1}/Z'_{c1} = 0.01$.

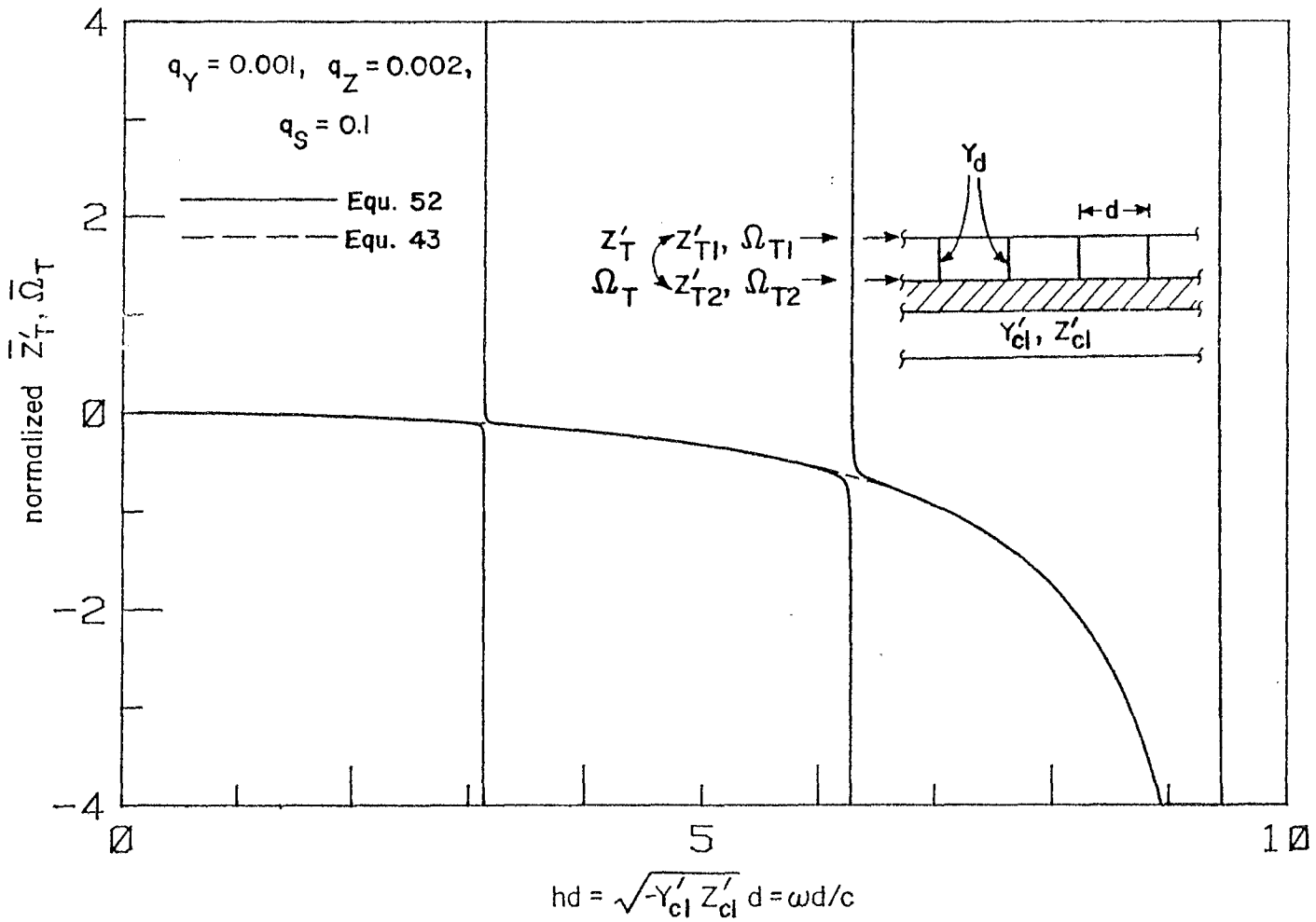

Figure 22. Normalized $\bar{Z}'_T$ and $\bar{\Omega}_T$ (normalized to their values when the cable shields are not bonded), based on the general Equation 52 and the approximated Equation 43, versus frequencies for $q_S = Z'_{c1} Y_d d = 0.1$, $q_Y = Y'_{c1}/Y'_{T1} = 0.001$ and $q_Z = Z'_{T1}/Z'_{c1} = 0.002$.

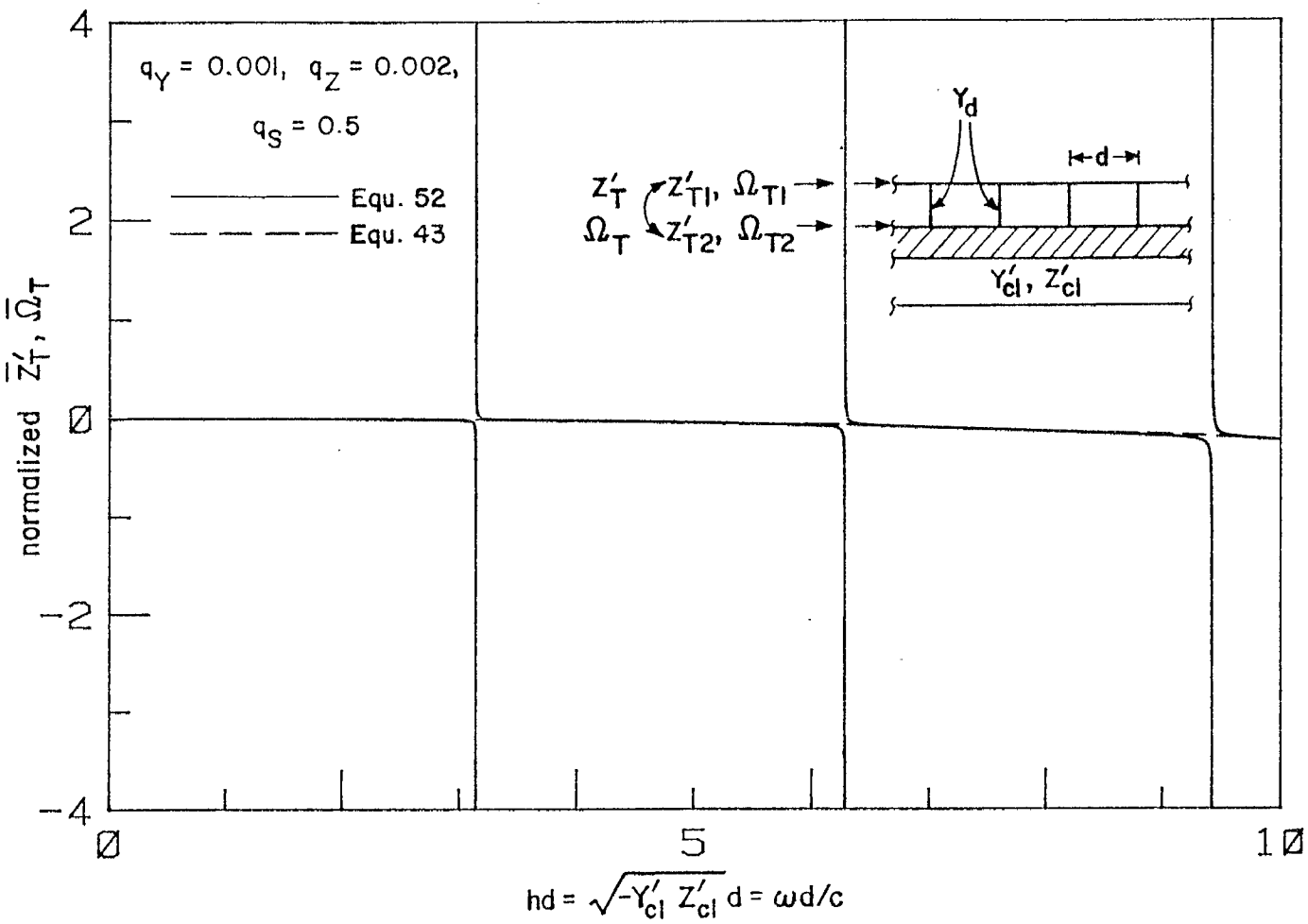

Figure 23. Normalized $\bar{Z}'_T$ and $\bar{\Omega}_T$ (normalized to their values when the cable shields are not bonded), based on the general Equation 52 and the approximated Equation 43, versus frequencies for $q_S = Z'_{c1} Y_d d = 0.5$, $q_Y = Y'_{c1}/Y'_{T1} = 0.001$ and $q_Z = Z'_{T1}/Z'_{c1} = 0.002$.

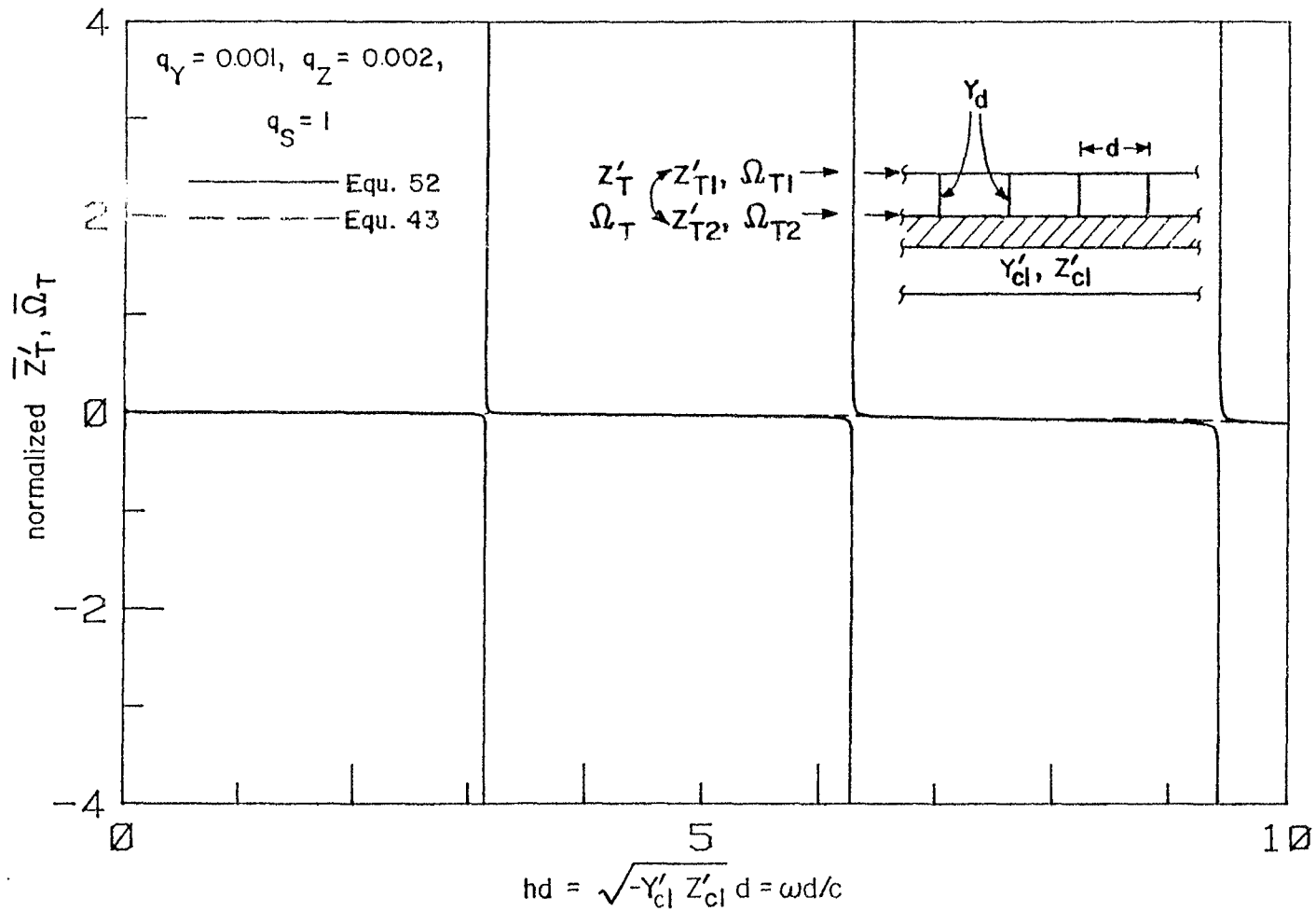

Figure 24. Normalized $\bar{Z}'_T$ and $\bar{\Omega}_T$ (normalized to their values when the cable shields are not bonded), based on the general Equation 52 and the approximated Equation 43, versus frequencies for $q_S = Z'_{c1} Y_d d = 1$, $q_Y = Y'_{c1}/Y'_{T1} = 0.001$ and $q_Z = Z'_{T1}/Z'_{c1} = 0.002$.

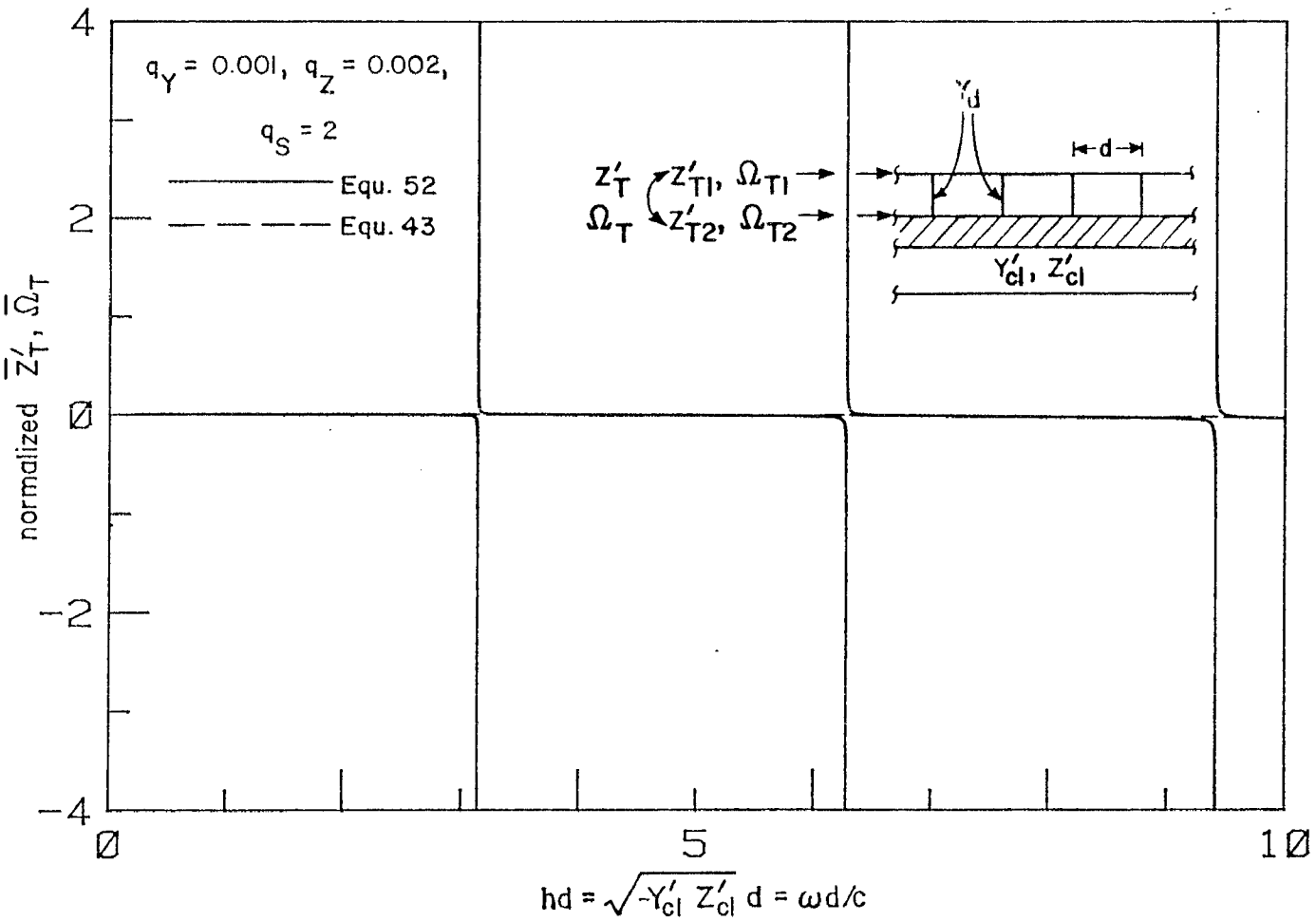

Figure 25. Normalized $\bar{Z}'_T$ and $\bar{\Omega}_T$ (normalized to their values when the cable shields are not bonded), based on the general Equation 52 and the approximated Equation 43, versus frequencies for $q_S = Z'_{c1} Y_d d = 2$, $q_Y = Y'_{c1}/Y'_{T1} = 0.001$ and $q_Z = Z'_{T1}/Z'_{c1} = 0.002$.

Pages 581 and 584 of Ref. 4). In the figures, the curves of the approximate Equation 43 are also given. The agreement between Equations 43 and 52 in the region where $\omega d/c$ is not close to $n\pi$ ($n = 1,2, \ldots$) is clearly shown even when hd is smaller or in the order of q_S. The reason they agree when $hd \lesssim q_S$ is simply because both Equations 43 and 52 have values in the order of q_Y or q_Z ($<< 1$). Because of this, probably one can lift the condition $hd >> q_S$ in Equation 53. From the figures one can draw the same conclusions as those of the discrete excitation case that the bondings improve the shielding effectiveness at certain frequency ranges while degrade it at others. In order to widen the frequency ranges for better shielding effectiveness, one may try to increase $Z'_1 Y_d$. Also one should not use a "d"-value which causes resonances (where $\omega d/c \simeq n\pi$, $n = 1,2, \ldots$) and thus seriously degrades the shielding effectiveness.

Equation 52 can also be rewritten in the following form:

$$\frac{\bar{Z}'_T}{Z'_{T2}} = \frac{\bar{\Omega}_T}{\Omega_{T2}} = \frac{Z'_{T1} + h^2/Y'_{T1}}{Z'_1 + h^2/(Y'_1 + qY_d/d)} \qquad (55)$$

where

$$q = \frac{q_1}{1 + dY_d Z'_1 (q_2 - q_1)/[(h^2 + Y'_1 Z'_1) d^2]} \qquad (56)$$

$$q_1 = (Z'_{T1} Y'_{T1} - Z'_1 Y'_1)/(Z'_{T1} Y'_{T1} + h^2) \qquad (57)$$

$$q_2 = \frac{\sin(d\sqrt{-Y'_1 Z'_1})/(d\sqrt{-Y'_1 Z'_1})}{[\cos(d\sqrt{-Y'_1 Z'_1}) - \cos(hd)]/[(h^2 + Y'_1 Z'_1) d^2/2]} \qquad (58)$$

Equation 55 can be easily represented by a circuit (Fig. 26). Under the assumption that the diffusion penetration is not important, the q-values are plotted in Figures 27 and 28 as functions of $hd \simeq \sqrt{-Y'_{c1} Z'_{c1}}\, d = \omega d/c$, with q_Z, q_Y and q_S as parameters. The values of the parameters in Figures 27

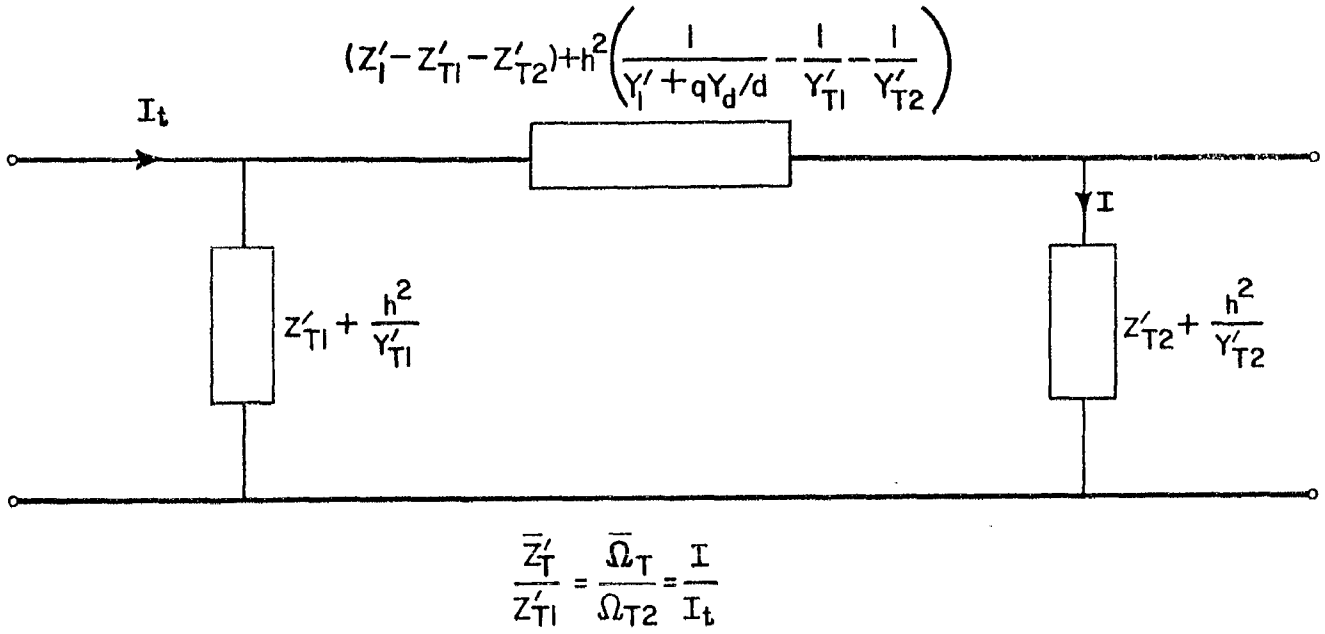

Figure 26. The general circuit for the calculations of $\bar{Z}_T'$ and $\bar{\Omega}_T$ of a double shield with periodic bondings.

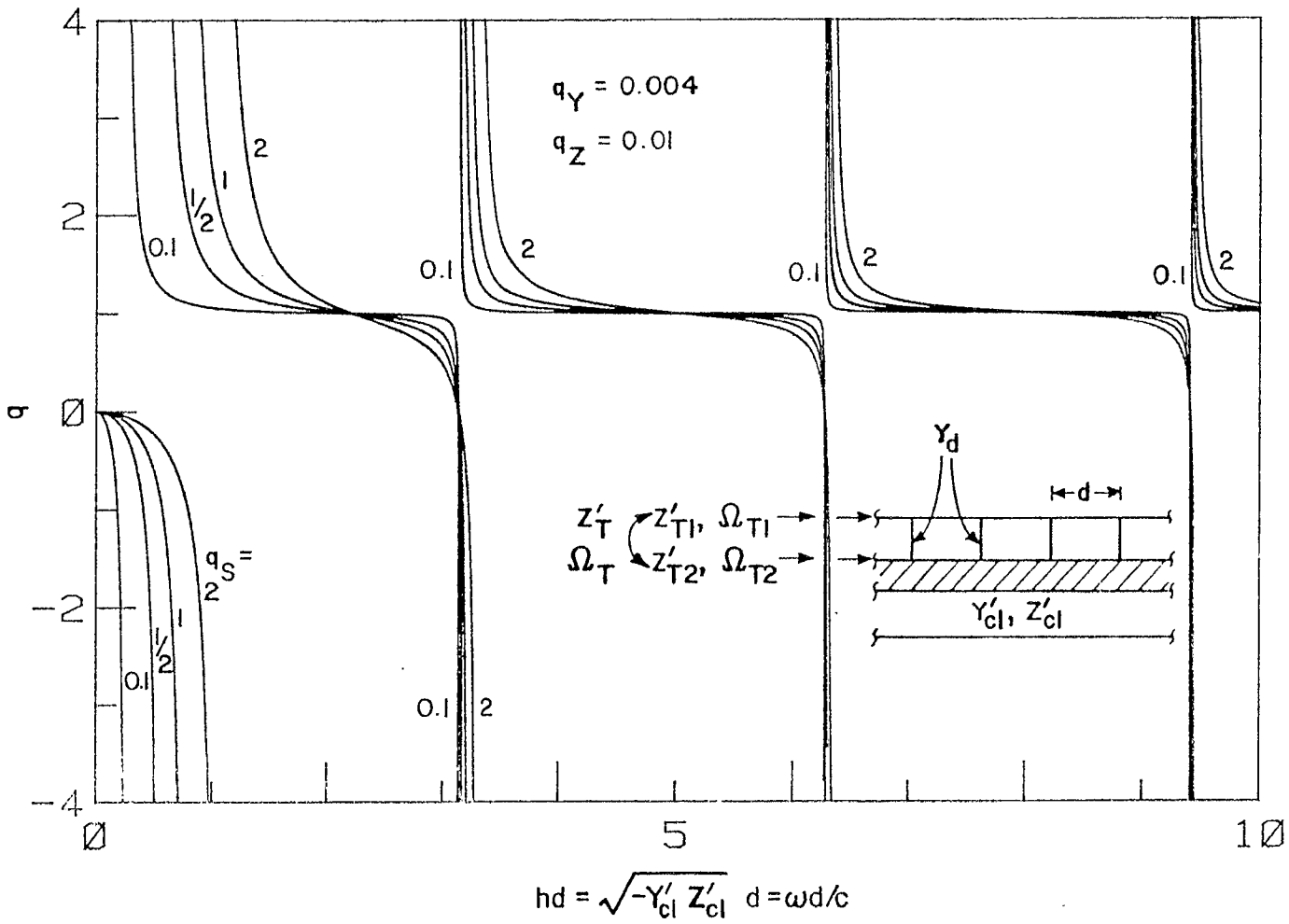

Figure 27. The values of "q", to be used in the circuit of Figure 26, versus frequencies for $q_Y = Y'_{c1}/Y'_{T1} = 0.004$, $q_Z = Z'_{T1}/Z'_{c1} = 0.01$ and various $q_S = Z'_{c1} Y_d d$.

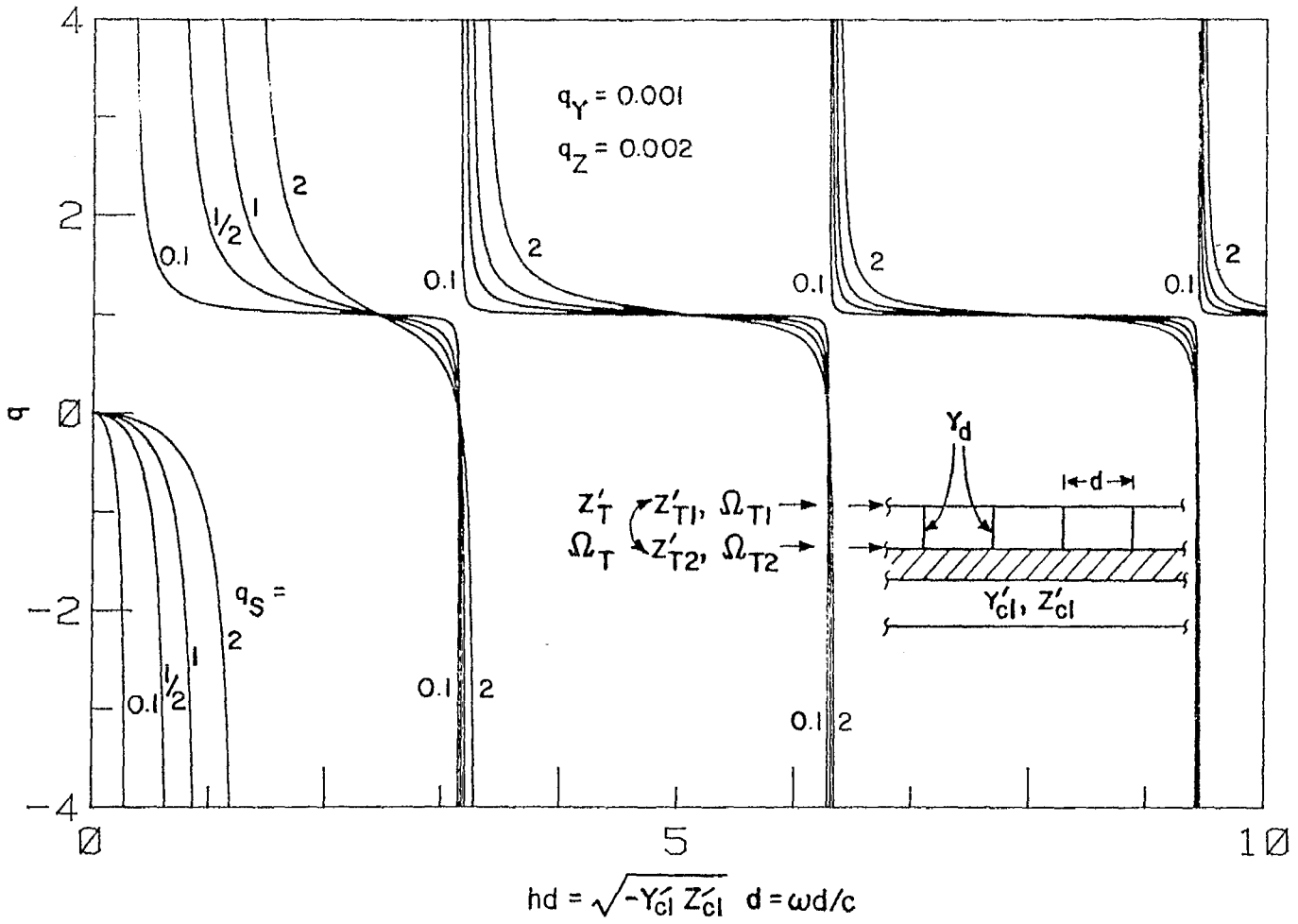

Figure 28. The values of "q", to be used in the circuit of Figure 26, versus frequencies for $q_Y = Y'_{c1}/Y'_{T1} = 0.001$, $q_Z = Z'_{T1}/Z'_{c1} = 0.002$ and various $q_S = Z'_{c1} Y_d d$.

and 28 are the same as those of Figures 18 through 25. From the figures, one can easily see that $q \simeq 1$ when Conditions 53 and 54 are satisfied; that is, Equation 55 reduces to Equation 43. This is another proof that the simplified Equation 43 can be used for Equation 52 or 55 when the Conditions 53 and 54 are satisfied.

IV. SUMMARY

In this section, the results of Sections II and III are summarized and some examples are worked out to show how the results can be used.

1. DISCRETE EXCITATIONS

When the outer shield of a double-shield configuration is coupled to a localized voltage and/or current source (Figs. 1 and 3), one may employ the Floquet theorem to the periodic transmission-line equations to determine the disturbances propagating down the bonded double shield. A passband-stopband structure in the dispersion relation between ω and k is observed (Eq. 8 and Fig. 6). In the stopbands the disturbances decay exponentially away from the penetration point, whereas in the passbands the disturbances oscillate persistently. In the stopband the decaying constant can be easily determined from the dispersion relation. Curves of the decaying constant are plotted in Figure 7. At low frequencies the decaying constants can be calculated from the simple approximate Equations 9 and 10.

a. Voltage source (V_o^s, see Figs. 3b and 4a)

The voltage source can be calculated from

$$V_o^s = I_{sc} Z_{T1} \tag{59}$$

where I_{sc} is the short-circuit current on the outermost surface of the double shield, and Z_{T1} is the localized transfer impedance of the outer shield. This voltage source gives rise to V_s' and I_s' which are the voltage- and current-sources exciting the wires inside the inner shield. By defining a combined effective transfer impedance per unit length Z_{TV}' and a combined effective charge transfer frequency per unit length Ω_{TV}' as

$$Z_{TV}' = V_s'/I_{sc}$$

$$\Omega_{TV}' = j\omega I_s'/I_{sc}$$

one can fully describe the coupling through the bonded double shield due to a voltage source V_o^s (or I_{sc}, see Eq. 59). Z'_{TV} and Ω'_{TV} are averaged over the period d via Equation 20. The averaged quantities $\overline{Z}'_{TV}$ and $\overline{\Omega}'_{TV}$ are given in Equation 21 and plotted in Figures 8 through 11 after normalized to their values for no bonding strap $(Z_{T1}Z'_{T2}(Z'_1/Y'_1)^{-1/2}/n_p$ and $Z_{T1}\Omega_{T2}Y'_1/n_p$, respectively, where $n_p = 1$ for Figure 3b and $n_p = 2$ for Figure 4, Z'_{T2} and Ω_{T2} are the coupling coefficients of the inner shield).

b. Current source (I_o^s, see Figs. 3b and 4b)

The current source can be calculated from

$$I_o^s = Q'_{sc}\Omega_{T1}^L \tag{60}$$

where Q'_{sc} is the short-circuit charge density on the outermost surface of the double shield and Ω_{T1}^L is the localized charge transfer frequency of the outer shield. This current source gives rise to different V'_s and I'_s (different from those due to V_o^s). By defining a combined effective transfer impedance Z_{TI} and a combined effective charge transfer frequency Ω_{TI} via

$$Z_{TI} = V'_s/(j\omega Q'_{sc})$$

$$\Omega_{TI} = I'_s/Q'_{sc}$$

one can describe the coupling through the bonded double shield due to a current source I_o^s (or Q'_{sc}, see Eq. 60). Z_{TI} and Ω_{TI} are also averaged via Equation 20. The averaged quantities $\overline{Z}_{TI}$ and $\overline{\Omega}_{TI}$ are given in Equation 26 and plotted in Figures 12 and 13 after normalized to their values for no bonding strap $(\Omega_{T1}^L Z'_{T2}/(n_p j\omega)$, $\Omega_{T1}^L\Omega_{T2}/(cn_p)$ respectively).

Figures 8 through 13 (or, more generally, Eqs. 21 and 26) show that the absolute values of the normalized transfer quantities are less than one (where the bonding straps improve the shielding effectiveness) at some frequency ranges and greater than one at the others. The figures also show that the transfer quantities become infinity at $\omega d/c \approx n\pi$ $(n = 1,2,3, \ldots)$. The transfer quantities, however, are not given in the stopbands (also see Figs. 6 and 7) where they are extremely small far away from the penetration point.

From the above observations, one concludes that in order to have a better shielding effectiveness, the periodic bonding should be employed such that the important part of the EMP spectrum lies inside the first stopband. This can generally be realized by choosing an appropriate d when Y_d and Z_1' are specified. Also, in order to have a broader first stopband and a greater decaying constant, one should try to make $Z_1'Y_d$ larger.

c. Examples

For a coaxial double shield with outer radius (b) = 5 cm and inner radius (a) = 3 cm, one has

$$Z_1' \simeq j\omega L_1' \simeq \frac{j\omega\mu_o}{2\pi} \ell n\left(\frac{b}{a}\right) \simeq 10^{-7} j\omega \quad (\Omega/m) \tag{61}$$

i.e.,

$$L_1' \simeq 10^{-7} \text{henry/m}$$

Also, suppose that highly conducting wires of radius t = 1 mm are to be used for bonding, then,

$$Y_d \simeq (j\omega L_d)^{-1} \simeq (j\omega)^{-1} \frac{2\pi}{\mu_o(b-a)} \frac{1}{\ell n(2(b-a)/t)} \tag{62}$$

$$\simeq 6.7 \times 10^7 (j\omega)^{-1} \quad (\Omega)^{-1}$$

i.e.,

$$L_d \simeq 1.5 \times 10^{-8} \text{henry}$$

Thus,

$$Z_1'Y_d \simeq 6.8 \ (m^{-1})$$

The question now arises as to the spacing d to be used. Take d = 0.6 m and 0.3 m as given in Table 1. Both cases give rather wide first stopbands which cover the important EMP spectrum. However, the case of d = 0.3 m gives a wider first stopband and a larger decaying constant (note that a decaying constant of $1(m^{-1})$ corresponds to an atteunation of 8.7 dB/m).

Another important quantity is $Z_1'Y_d$, which should be made as large as possible for better shielding effectiveness. If the double shield is coaxial, one can use a smaller (b - a) to obtain a larger $Z_1'Y_d$ (Eqs. 61 and 62). The case of b = 4 cm and d = 0.6 m is also given in Table 1. From the table, it is observed that the first stopband is wider and the decaying constant is larger for b = 4 cm, d = 0.6 m than the case for b = 5 cm, d = 0.6 m.

TABLE 1. EXAMPLES OF BONDED COAXIAL-CABLE SHIELDS

	b = 5cm, a = 3cm, t = 1mm (L_1' = .1μh/m, L_d = 15 nh)		b = 4cm, a = 3cm, t = 1mm (L_1' = 57 nh/m, L_d = 6 nh)
Period of Bondings	d = .3m	d = .6m	d = .6m
$Z_1'Y_d$ (= L_1'/L_d)	$6.7m^{-1}$		$9.6m^{-1}$
1st Stopband	0 ↔205 MHz	0 ↔137 MHz	0 ↔160 MHz
|Im(k)| ,Below 10 MHz	$4.4m^{-1}$	$2.9m^{-1}$	$3.4m^{-1}$

2. DISTRIBUTED EXCITATIONS

Given the distributed transfer parameters of both the inner and outer shields (Figs. 2 and 14), the effective overall transfer parameters of the double shield can be represented by simple circuit diagrams. These circuit diagrams are summarized below.

a. Schelkunoff's circuit (Ref. 6)

When the shields are solid tubular conductors whose skin depths, linear cross-sectional dimensions and the period of the bonding straps are much smaller than the wavelength of the EMP disturbance, the effective transfer impedance of the double shield Z_T' (the effective charge transfer frequency Ω_T is, of course, zero) is independent of the bonding straps and can be calculated from the circuit depicted in Figure 15 or from Equation 30. The circuit elements in Figure 15 and Equation 30 are given in Equations 28 and 29, and also Equations 32 through 36 for some special cases. The circuit can be easily extended for a N-surface solid tubular shield with N > 2.

b. Casey's circuit (Ref. 7)

When (a) the skin depths of the shields are much greater than their thickness ($\delta >> \Delta$, thin shields), (b) the linear cross-sectional dimensions of the double shield are much less than the wavelength of the EMP disturbance ($hb \simeq \sqrt{-Y_1'Z_1'}\, b << 1$), and (c) there is no bonding strap, then, Z_T' and Ω_T can be calculated from the circuit of Figure 16 or from Equation 42. The circuit elements in the figure and the equation are given in Equations 37, 38, 39 and 41.

When the shields are not thin, the circuit of Figure 17 (called the generalized Casey's circuit) can be used to replace that of Figure 16 for calculating Z_T' and Ω_T. Equation 42 is still applicable, except that the circuit element Z_1', originally given by Equation 41, becomes

$$Z_1' = Z_{a1}' + Z_{b2}' + Z_{c1}'$$

Here, Z_{a1}' and Z_{b2}' are defined in a broader sense than Equation 28 to include all kinds of penetrations. Both circuits in Figures 16 and 17 can also be easily extended to describe a N-surface shield with N > 2.

c. General circuit

When there are periodic bondings connecting the shields, $\overline{Z}_T'$ and $\overline{\Omega}_T$ (the average values of Z_T' and Ω_T over the period of the bondings) can be calculated from the circuit in Figure 26 or from Equation 55 (or equivalently, Equation 52). The constant "q" (qY_d/d may be named the effective shunt admittance per unit length of the bondings) in Equation 55 and Figure 26 is a complicated function of the shield and bonding parameters (Eqs. 56 through 58). However, when the conditions given in Equations 53 and 54 are met, q is approximately equal to 1, i.e., Equation 55 reduces to Equation 43. The truth of this statement is further supported by the curves in Figures 27 and 28 for "q" and the curves in Figures 18 through 25 for the normalized $\overline{Z}_T'$ and $\overline{\Omega}_T$ (normalized to their corresponding values for no bonding strap, i.e., Equation 55 with q = 0). Actually, in Figures 18 through 25, the curves of Equation 43

agree with those based on the exact Equation 55 even in the region where $hd \lesssim q_S$ (i.e., the condition $hd >> q_S$ in Equation 53 is violated, and q is quite different from one as shown in Figures 27 and 28),, provided hd is not close to $n\pi$. One thus concludes that when $q_S \gtrsim 0.1$, $|hd - \sqrt{-Y_1'Z_1'}\, d\,| << 1$ and hd is not close to $n\pi$ ($n = 1,2, \ldots$) Equation 43 or the circuit in Figure 26 with $q = 1$ is a good approximation for calculating $\overline{Z}_T'$ and $\overline{\Omega}_T$.

From the results presented, one concludes that in order to shield against the distributed excitations more effectively, the periodic bondings should be implemented in such a way that $Z_{c1}'Y_d$ is large and $\omega d/c < \pi$ for the important parts of the EMP spectrum.

d. Examples

Consider a coaxial double shield (Fig. 2) with outer radius b = 5 cm, inner radius a = 3 cm and with highly conducting bonding straps of radius t = 1 mm. Also, take the practical values $q_Y = Y_{c1}'/Y_{T1}' = 0.004$ and $q_Z = Z_{T1}'/Z_{c1}' = 0.01$. Then,

$$Z_{c1}'Y_d \simeq 6.7\ (m^{-1})$$

from which

$$q_S = Z_{c1}'Y_d d \simeq \begin{cases} 2 & \text{for } d = 0.3\ m \\ 1 & \text{for } d = 0.15\ m \end{cases}$$

From Figures 20 and 21, one immediately sees that the normalized transfer functions are less than 0.1 (i.e., the bonding straps reduce the EMP penetration by more than 20 dB) for

$$\text{frequencies} < \begin{cases} 470\ \text{MHz} & \text{when } d = 0.3\ m \\ 940\ \text{MHz} & \text{when } d = 0.15\ m \end{cases}$$

Both 470 MHz and 940 MHz are extremely high to be important.

However, if the bonding straps between the coaxial double shield give a much smaller $Z'_{c1}Y_d$ value, say,

$$Z'_{c1}Y_d \approx 0.67\ m^{-1}$$

then, when d = 0.15 m is used the same quality in the shielding effectiveness as that of $Z'_{c1}Y_d \approx 6.7\ m^{-1}$ and d = 0.15 m can be obtained only for frequencies up to at most 300 MHz (see Fig. 18). Thus, bonding straps with greater $Z'_{c1}Y_d$ are preferred.

REFERENCES

[1] "B-52 Survivability as a Standoff Cruise Missile Carrier, Final Report of the Team B Study Effort, Vol. II - Technical Report," Air Force Weapons Laboratory, Kirtland AFB, NM, January 1980.

[2] Lam, J., "Propagation Characteristics of a Periodically Loaded Transmission Line," Interaction Notes, Note 302, Air Force Weapons Laboratory, Kirtland AFB, NM, November 1976.

[3] Gradshteyn, I.S., and I.W. Ryzhik, Table of Integrals, Series and Products, Academic Press, New York and London, 1965.

[4] Lee, K.S.H., Editor, EMP Interaction: Principles, Techniques and Reference Data, EMP Interaction Notes, Note 2-1, Air Force Weapons Laboratory, Kirtland AFB, NM, 1979.

[5] Lee, K.S.H., and C.E. Baum, "Application of Modal Analysis to Braided-Shield Cables," IEEE Trans. on EMC, Vol. EMC-17, No. 3, August 1975, also Interaction Notes, Note 132, Air Force Weapons Laboratory, Kirtland AFB, NM, January 1973.

[6] Schelkunoff, S.A., "The Electromagnetic Theory of Coaxial Transmission Lines and Cylindrical Shields," Bell Syst. Tech. J., Vol. 13, October 1934.

[7] Casey, K.F., "On the Effective Transfer Impedance of Thin Coaxial Cable Shields," IEEE Trans. on EMC, Vol. EMC-18, No. 3, August 1976, also, Interaction Notes, Note 267, Air Force Weapons Laboratory, Kirtland AFB, NM, March 1976.